Biofilm formation of *Listeria monocytogenes* 15G01, a persistent isolate from a seafood-processing plant, is influenced by inactivation of multiple genes belonging to different functional groups

Jessika Nowak[1,2], Sandra B. Visnovsky[3], Andrew R. Pitman[5], Cristina D. Cruz[1,4], Jon Palmer[2], Graham C. Fletcher[1], Steve Flint[2]

[1] The New Zealand Institute for Plant and Food Research Limited, Mt Albert, Auckland, New Zealand

[2] Institute of Food, Nutrition and Human Health, Massey University, Palmerston North, New Zealand

[3] The New Zealand Institute for Plant and Food Research Limited, Lincoln, New Zealand

[4] Drug Research Program, Division of Pharmaceutical Biosciences, Faculty of Pharmacy, P.O. Box 56, FI-00014 University of Helsinki, Finland

[5] The Foundation for Arable Research, Christchurch, New Zealand

Abstract

Listeria monocytogenes is a ubiquitous foodborne pathogen that results in a high rate of mortality in sensitive and immunocompromised people. Contamination of food with *L. monocytogenes* is thought to occur during food-processing, most often as a result of the pathogen producing a biofilm that persists in the environment, and acting as the source for subsequent dispersal of cells onto food. A survey of seafood-processing plants in New Zealand identified the persistent strain 15G01, which has a high capacity to form biofilms. In this study, a transposon library of *L. monocytogenes* 15G01 was screened for mutants with altered biofilm formation, assessed by a crystal violet assay, to identify genes involved in biofilm formation. This screen identified 36 transposants that showed a significant change in biofilm formation compared to the wild-type. The insertion sites were in 27 genes, of which 20 led to decreased biofilm formation and seven to an increase. Two insertions were in intergenic regions. Annotation of the genes suggested that they are involved in diverse cellular processes, including stress response, autolysis, transporter systems and cell wall/membrane synthesis. Analysis of the biofilms produced by the transposants using scanning electron microscopy and fluorescence microscopy showed notable differences in the structure of the biofilms when compared with the wild-type. In particular, inactivation of *uvrB* and *mltD* produced coccoid-shaped cells and elongated cells in long chains, respectively, and the *mgtB* mutant produced a unique biofilm with a sandwich structure which was reversed to the wild-type level upon magnesium addition. The *mltD* transposant was successfully complemented with the wild-type gene, whereas the phenotypes were not or only partially restored for the remaining mutants.

Importance

The major source of contamination of food with *Listeria monocytogenes* is thought to be due to biofilm formation and/or persistence in food-processing plants. By establishing as a biofilm, cells become harder to eradicate due to their increased resistance to environmental threats.

Understanding the genes involved in biofilm formation and their influence on biofilm structure will help identify new ways to eliminate harmful biofilms in food processing environments. To date multiple genes have been identified as involved in biofilm formation of *L. monocytogenes*, however, the exact mechanism remains unclear. This study has identified four genes associated with biofilm formation in a persistent strain. Extensive microscopic analysis illustrated the effect of the disruption of *mgtB*, *clsA*, *uvrB* and *mltD* and the influence of magnesium on the biofilm structure. This work strongly suggests an involvement in biofilm formation for the four genes and provides a basis for further studies to analyse gene regulation to assess the specific role of these biofilm-associated genes.

Introduction

The foodborne pathogen *Listeria monocytogenes* is a serious health threat to immunocompromised people, the elderly, pregnant women and unborn and newborn babies (1), with a high mortality rate (up to 30%) in those groups (2). *L. monocytogenes* is ubiquitous in the environment, with contamination of food usually occurring during processing rather than being present in raw food (3, 4). The breadth of foods contaminated with *L. monocytogenes* is extensive, and includes ready-to-eat meat and seafood as well as vegetables and fruit (5).

L. monocytogenes is motile across a broad range of temperatures and has the capacity to adapt quickly to environmental changes to secure its survival. It can grow over a broad temperature range and survive freezing temperatures (6). *L. monocytogenes* can tolerate some degree of low pH, but is not as acid-tolerant as some other foodborne pathogenic bacteria, i.e. E. coli O157:H7. It is also capable of surviving in high salt concentrations up to 11.5 % (6). All these attributes contribute to the adaptability of this pathogen and impede its control when encountered in food-processing environments.

Surface attachment and biofilm formation are important to the environmental persistence of *L. monocytogenes* (7). A biofilm is a community of cells that exists in a sessile lifestyle rather than a planktonic one in order to use resources more efficiently and to resist environmental threats. Cells in a biofilm are attached to each other and to a surface. They are held together by an extracellular polymeric matrix that consists of DNA, proteins, lipopolysaccharides and other substances that contribute to its stability and act as a protective barrier. For *L. monocytogenes*, the capacity to form biofilms in so-called ‘harbourage’ sites, enables the pathogen to establish itself and to act as a source for subsequent dispersal of single cells. Management of *L. monocytogenes* is further impaired because biofilm cells are more resistant to cleaning agents and sanitisers (8) as well as antibiotics (9). As a result, *L. monocytogenes* is able to contaminate surfaces as well as food products.

Transposon mutagenesis has proven to be a successful tool for identification of genes involved in biofilm formation in *L. monocytogenes* (10, 11). As a result, to date, four research groups have successfully identified genes involved in biofilm formation of *L. monocytogenes* using the Himar1-based transposition system (12-15). The majority of the identified genes were associated with biosynthesis or motility. This transposition system has also been used to identify the genetic factors underlying other phenotypic changes, such as desiccation survival or nisin-sensitivity (16, 17).

A survey of seafood-processing plants in New Zealand identified four persistent strains (persisted in factories for at least 6 months), classified by their unique pulsotypes (18). One of these pulsotypes (5132), represented by *L. monocytogenes* 15G01, was shown to have a high capacity to form biofilms in *in vitro* assays (18-20). Further genomic studies revealed that *L. monocytogenes* 15G01 (lineage II genome) belongs to the sequence type ST-321, determined using MLST, and is lacking the φtRNA-Ser prophage (20). This isolate exhibited low invasion in mammalian cell cultures (20), which is linked to truncation of the primary virulence factor internalin A (InlA) (21). As the capacity to form biofilms is believed to be a major contributing factor in persistence of *L. monocytogenes* and subsequent contamination of food in food-processing premises, a library of mutants of *L. monocytogenes* 15G01, previously generated using the Himar1 mariner-based transposition system (22), was screened for mutants with altered biofilm formation using the crystal violet assay. This study aimed to reveal additional genes in *L. monocytogenes* 15G01 that are associated with biofilm formation and to further characterise the role of these genes through visualisation of the structure by using scanning electron and fluorescence microscopy to visualise the structure of the altered biofilms.

Results

An *in vitro* biofilm assay identified multiple mutants that have either greater or lower biofilm formation than the wild-type

A set of 4,500 mutants of a transposant library of approximately 6,500 mutants of *L. monocytogenes* 15G01, created with the mariner transposition system, was screened at 30°C in MWB for mutants with altered biofilm formation using the CV assay (a set of 2000 mutants has been analysed previously (20). These conditions were used as they were previously shown to induce biofilm formation in *L. monocytogenes* 15G01 (19). In total, 36 mutants were found with greater (10 mutants) or lower (26 mutants) biofilm formation ability under these conditions compared to the wild-type (Table 2), with the average OD_{595nm} of the mutants being at least 2 SD below or above the average OD_{595nm} value (1.197) of the wild-type *L. monocytogenes* 15G01. The growth of the mutants was compared to the growth of the wild-type strain in MWB during the screen to confirm that the altered biofilm formation observed was not due to differences in the ability of the mutants to grow in this media and only mutants showing equal or higher OD_{595nm} than the wild-type after 48 h were included.

Characterisation of the transposon insertion sites in mutants with altered biofilm formation identified 27 loci potentially involved in this process

Nested semi-arbitrary PCR enabled the amplification of the genome sequences flanking the transposons in the 36 mutants. DNA sequencing of the flanking regions and subsequent BlastN and megablast comparisons of the sequences with the genome of reference strain *L. monocytogenes* EGD permitted the locations and directions of the insertions in 15G01 to be estimated for all mutants with identification of the exact insertion sites for 28 mutants (Table 2). Transposon insertions seemed to predominantly occur in the second half of the genome raising doubts as to the random nature of transposition (Figure S3a). In the 36 mutants examined, 27 genes were disrupted by a transposon insertion, with six loci disrupted in two independent

mutants and one disrupted in three independent mutants (Table 2). Two mutants had an insertion of the transposon in an intergenic region (Table 2) and a further two mutants insertions in genes that were not present in the reference genome of *L. monocytogenes* EGD, but in the parental strain *L. monocytogenes* 15G01.

Functional analysis of the disrupted genes identified multiple functional groups are involved in biofilm formation in *L. monocytogenes* 15G01

Comparison of the disrupted genes in each of the mutants affected in biofilm formation with homologous genes in *L. monocytogenes* EGD and other *L. monocytogenes* strains in the GenBank database divided them into seven diverse functional groups (Table 2). Of particular note, five genes annotated as being involved in cell wall/membrane synthesis or integrity were identified, including genes encoding a putative peptidoglycan bound protein disrupted in three mutants that had low biofilm formation, cardiolipin synthetase (designated as *clsA*), disrupted in two mutants with greater biofilm formation and the glycosyltransferase LafA in two mutants with low biofilm formation.

Genes involved in transport systems, stress response, autolysis and motility also influenced biofilm formation, including a gene predicted to encode a P-type $Mg^{(2+)}$ transport ATPase (designated as *mgtB*) and a gene annotated as encoding the ABC transporter permease protein EscB, which were both disrupted in two mutants. Disruption of the P-type $Mg^{(2+)}$ transport ATPase resulted in decreased biofilm formation, whilst the insertion of the transposon into *escB* resulted in increased biofilm formation.

Complementation of selected genes confirms a role for *mltD* in biofilm formation of *L. monocytogenes* 15G01

Four mutants (33E11, 34F11, 39G5 and 44D3) were examined further to confirm the role of the disrupted genes in biofilm formation of *L. monocytogenes* 15G01. The first, the *clsA* mutant

149 (34F11), was selected because this gene had been disrupted in multiple mutants with increased
150 biofilm formation and the *clsA* gene was known to be involved in biofilm formation of other
151 bacterial species (23-25). The *uvrB* mutant (33E11) was selected as multiple mutants in the
152 excision nuclease ABC subunit B were identified in the screen and *uvrB* is part of an operon
153 with *uvrA*, which, when disrupted in *L. monocytogenes* in a previous study, showed increased
154 biofilm formation at 15°C (15). The *mltD* mutant (39G5) was studied because it was predicted to
155 affect autolysis, which has been implicated in changes in biofilm formation *in L. monocytogenes*
156 (26, 27) and other bacteria (28), whilst the *mgtB* mutant (44D3) was included because it has
157 also been disrupted in multiple mutants and has not been associated with biofilm formation in *L.*
158 *monocytogenes* before.

159 Growth curves of the selected 36 mutants in MWB at 30°C were then produced by manual
160 measurements to further examine growth behaviour (Table S1 and Figure S1) in the presence
161 of erythromycin (transposon contains erythromycin resistance gene). Additionally, growth
162 studies with an automated plate reader were carried out for the four selected mutants without
163 selective antibiotics to further rule out the possibility that the changes in biofilm formation were
164 due to impaired growth (Figure S2). The two mutants 39G5 and 44D3 formed cell aggregates
165 during growth which is reflected by the high OD_{600nm} values, however, growth pattern was not
166 affected. 39G5 had an extended exponential phase compared to the other strains, however all
167 five examined strains were in stationary phase at 48 h, the time point at which biofilm formation
168 was measured.

169 Complementation studies were subsequently carried out on the four mutants. In these studies,
170 introduction of the pIMK vector containing the wild-type *mltD* gene into the *mltD* mutant resulted
171 in the restoration of biofilm formation to levels produced by the wild-type (Figure 1). Conjugation
172 of the empty vector into this mutant had no obvious effect on biofilm formation (Figure 1). These
173 data confirmed that the change in biofilm formation in the *mltD* (a homologue of the

peptidoglycan hydrolase *murA*) mutant was a result of inactivation of the gene. Thus, *mltD* is required for biofilm formation in *L. monocytogenes* 15G01.

In contrast to the successful complementation of the *mltD* mutant (39G5), introduction of the pIMK vector containing the wild-type *uvrB* gene into the *uvrB* mutant only partially restored (41.7 %) the wild-type phenotype (Figure 1), whilst attempts to complement the *mgtB* and *clsA* mutants (44D3 and 34F11) using a similar process failed to restore the wild-type phenotype altogether (data not shown).

Microscopy confirmed that the *mltD* mutant (39G5) has a dramatic loss in both viable and non-viable cells

All the selected mutants were included in microscopic analysis to assess changes in phenotype despite the failure to complement a number of the mutations. Fluorescence microscopy showed that after 48 h incubation of the mutants on polystyrene surfaces in MWB at 30°C, all appeared to show some differences in the structure of their biofilms when compared to the wild-type (Figure 2). The biofilm of the *mltD* mutant (39G5) (Figure 2 d) consisted of a few (mainly individual) cells, which seemed to be elongated and in chains. The lack of visible cells (whether alive or dead) was consistent with the low biofilm formation observed in the initial screen. The biofilm produced by the *mgtB* mutant (44D3) also contained few live cells, although it did appear to have a cloudy structure under fluorescence (Figure 2 e). Consistent with this, there appeared to be greater numbers of dead cells associated with the biofilm produced by the *mgtB* mutant. The *uvrB* mutant (33E11) was a low biofilm former and exhibited only sparse biofilm formation after 48 h (Figure 2 c), which was consistent with the approximately 80% reduction in biofilm formation observed in *in vitro* assays. The *clsA* mutant (34F11) showed a biofilm with a high number of living cells, but also showed a higher amount of dead, red-stained cells (Figure 2 b).

SEM was used to analyse further the structure of the biofilms produced by the mutants after growth of the bacteria on stainless steel (SS) coupons coated with mussel juice for 7 d at 30°C. A SS coupon coated with mussel juice was used as a control and organic debris was clearly visible (Figure 3 k and l). Bacterial cells attached and formed biofilms on the coupons preferably where organic debris of the mussel juice was present (Figure 3 i and j).

SEM images of 39G5 confirmed the long chain phenotype with some elongated cells (Figure 3 g and h). Transposon mutant 33E11 was a low biofilm former and exhibited only sparse biofilm formation on SS coupons after 7 d although extracellular matrix was present. 33E11 appeared to have a different cell morphology compared to the wild-type with coccoid-shaped rather than rod-shaped cells (Figure 3e and f). Transposon mutant 34F11 identified as a high biofilm former in both the microtitre plate screening test and under the fluorescence microscope, also exhibited greater biofilm formation on the SS coupons compared to the wild-type (Figure 3 c and d). In addition, 34F11 exhibited an extensive thread structured biofilm attached to organic mussel debris (Figure 3 d).

Confocal analysis reveals a unique sandwich structure for the biofilm of the *mgtB* mutant

The influence of magnesium on the biofilm structure was investigated using confocal analysis. COMSTAT was used to calculate biomass, roughness and maximum and average thickness of the biofilms (Table 3).

Isosurface images of the biofilms stained with SYTO 9 were generated with Imaris (Bitplane, Zurich, Switzerland). The wild-type control formed microcolonies on glass after 7 d incubation in MWB at 30°C (Figure 4 g and h). In contrast to the CV assay (Figures 4 a and b), where magnesium addition did not alter biofilm amount significantly, biomass was reduced in the presence of 5 mM Mg^{2+} for the wild-type when analysed with CLSM. However, maximum thickness and average thickness of the biomass remained the same when analysed with CLSM. It is possible that magnesium led to increased production or stabilisation of extracellular

polymeric substance (which is not detected by CLSM) for the wild-type. In addition, biofilms were formed on two different surfaces (polystyrene and glass), which could have also contributed to the observed differences.

As the differences for the biofilm mass in the presence of 5 mM Mg^{2+} was greatest when *mltD* mutant 39G5 was incubated at 37°C (Figure 4 b), this temperature was used for the CLSM analysis. Magnesium presence led to a decrease in biofilm and attached cells for 39G5 after 7 d incubation at 37°C (Figure 4 e and f). This was also observed with the CV assays after 48 h (Figures 4 a and b). Maximum thickness and average thickness were more than halved in the presence of 5 mM Mg^{2+} (46.71 % and 40.84 % of the thicknesses without additional magnesium, respectively) (Table 3).

44D3 (*mgtB* mutant) produced more biofilm mass in the presence of 5 mM Mg^{2+} compared with 1.67 mM Mg^{2+} and less biomass than the wild-type when grown in MWB (1.67 mM Mg^{2+}) (Table 3), which is in line with the observations made with the CV assay (Figure 4 a). Calculations with COMSTAT revealed double maximum thickness for the biofilm of 44D3 compared with biofilms formed by the wild-type and 44D3 in the presence of 5mM Mg^{2+} (Table 3). This suggests that Mg^{2+} restored the wild-type phenotype for the *mgtB* mutant (44D3) (Figure 4 g–k, Table 3). Mutant 44D3 produced a unique sandwich structure for the biofilm (Figure 4 j) with monolayers of bacterial cells at the top and bottom and EPS or fluid in between. This structure has, to the best of our knowledge, not been reported for a biofilm before. In the presence of 5 mM Mg^{2+}, 44D3 produced a biofilm similar in structure to the wild-type (Figure 4 i and k) further strengthening the hypothesis of restoration of the wild-type's phenotype.

The *mltD* mutant (39G5) was defective in autolysis, motility as well as biofilm formation

Inactivation of *mltD* (*murA*-homologue) has previously been shown to result in loss of motility in *L. monocytogenes* (27). Consistent with these findings, the *mltD* mutant created in this study exhibited no motility (Figure 5 b), which was restored upon gene complementation (Figure 5 b).

248 The Triton X-100 induced autolysis rate was reduced for the *mltD* mutant compared to the wild-
249 type (Figure 5 a), confirming the direct involvement in autolysis.

250 Furthermore, the *mltD* mutant, 39G5, produced less biofilm than the wild-type at 30°C but more
251 than the wild-type at 37°C. At both temperatures the presence of magnesium (5 mM) reduced
252 biofilm production to a minimum when measured with the CV assay and by CLSM. Attachment
253 studies revealed that the presence of magnesium did not alter the attachment ability of 39G5,
254 suggesting that magnesium influences the biofilm maturation process rather than surface
255 characteristics or initial attachment (Figure S5).

256 Observations of planktonic cells as well as biofilm cells in the present study using fluorescence
257 microscopy (Figure 2) and SEM (Figure 3 g and h) showed a high number of elongated cells in
258 long chains for the *mltD* mutant.

259 The *mltD* mutant was found to produce increased cell aggregation, which interfered with optical
260 density measurements for growth behaviour. However, cell counts after 24 h growth were
261 similar to the wild-type levels (>9.0 $\log_{10}$ CFU/mL) (Table S1).

262 **Discussion**

263 This study identified 27 genes that are involved in biofilm formation in *L. monocytogenes*
264 *15G01*. Four other research groups have also used Himar1 transposon mutagenesis to identify
265 genes involved in biofilm formation in *L. monocytogenes* (12-15). In each case, a large number
266 of loci were reportedly associated with biofilm formation. Many of the loci were only identified in
267 a single study, however, probably because different isolates and different assay conditions were
268 used. For example, Piercey, et al. (15) performed the assays at 15°C while other groups used
269 higher temperatures (32°, 35° or 37°C). We opted to carry out our analysis at 30 and 37°C even
270 though food processing plants operate at a lower temperature. These temperatures were

chosen for this high throughput screen to identify potential biofilm associated genes in a timely manner as lower temperature require longer incubation time due to slower growth rate.

All studies, including this one, showed that a transposon insertion in *lafA* (gene ID lmo2555 in *L. monocytogenes* EGDe), a gene encoding a glycosyltransferase required for membrane development, caused a reduction in biofilm formation (29). Other genes identified by us and other research groups are genes encoding for sortase A, a peptidoglycan linked protein (LPXTG) and the flagella protein FlaA (13). The detection of common genes associated with changes in biofilm formation under such variable conditions suggests that they are critical to biofilm formation regardless of the environmental conditions the bacterium experiences.

This study revealed the probably involvement of *uvrB* in biofilm formation. Piercey, et al. (15) identified *uvrA* (located in the same operon as *uvrB*) was also associated with biofilm formation. Our research group as well as Piercey, et al. (15) used a serotype 1/2a strain isolated from a processing plant to generate the transposon library.

Ouyang, et al. (14) and Alonso, et al. (12) both generated a mutant library using *L. monocytogenes* 10403S and Chang, et al. (13) created a library of *L. monocytogenes* Scott A mutants. The *uvrAB* cluster was not identified as involved in biofilm formation in these other studies, suggesting that either the regulatory cascades controlling biofilm formation may be specific to certain environmental triggers or that they may be influenced by genetic variability between strains or serotypes.

Transporter systems are essential in living organisms. The transition from a planktonic to a sessile lifestyle requires changes in metabolism and energy generation as resources within biofilms become scarce (30). Thus, during the screening of the *L. monocytogene*s 15G01 mutants, it was not surprising to identify seven genes involved in these broad processes that influence biofilm formation.

One transporter system of particular interest is the P-type ATPase which takes up Mg^{2+} upon ATP-hydrolysis (MgtB). Previous studies showed that magnesium deprivation triggers biofilm formation (31) and temperature-dependent expression (32) of *mgtB* is regulated by the PhoP/PhoQ two component system in Gram-negative bacteria (33, 34). However, knowledge about the function of this P-type ATPase in Gram-positive bacteria, in particular *L. monocytogenes*, is limited. No data about the involvement of *mgtB* in biofilm formation are currently available. According to Nielsen, et al. (35) *mgtB* (lmo2689) is regulated by the two component system CesRK. CesR binding boxes were found upstream of this *mgtB* gene which suggests direct control of *mgtB*. *mgtB* is part of an operon including genes encoding for cell division proteins (i.e., *ftsW*, Figure S3b) which are also regulated by CesR (35). CesRK is associated with virulence (36), ethanol sensitivity and antibiotic sensitivity (37). The transposon insertion in the *mgtB* gene (44D3) resulted in the production of a low biofilm phenotype in this study, suggesting an involvement of *mgtB* in biofilm formation of *L. monocytogenes*. The involvement of *mgtB* in biofilm formation has also been shown for *Cronobacter sakazakii* (38), where a disruption of *mgtB* led to a 77% reduction in biofilm mass. Other magnesium transporters (MgtE) have also been shown to be involved in biofilm formation or potentially even in virulence (39). Of particular interest in this study was the observed sandwich structure of the biofilm formed by 44D3 with static monolayers at the top and bottom and movement in the fluid in between (Figure 4). Similarly, (40)also observed movement in the fluid in hollow structures of the biofilm when analysing it with CLSM. This is the first time that such a biofilm structure has been reported. Magnesium has been shown to influence biofilm formation in other bacterial species (31, 41), where high magnesium concentrations (50 mM and higher) led to reduced biofilm formation in *Bacillus subtilis* and *Bacillus cereus* (41) without affecting the growth. However, lower concentration of 5 mM and 10 mM led to an increase in biofilm formation of *B. subtilis* in the same study. Other studies showed that Mg^{2+} presence led to increased attachment of *P. fluorescence* cells to glass (42), but, on the other hand, Mg^{2+} limitation resulted

in increased biofilm formation in *Pseudomonas aeruginosa* through repression of the *retS* gene which is responsible for EPS biosynthesis (Mulcahy and Lewenza 2011). Although findings are contradictory, it is clear that magnesium plays a vital role in biofilm formation and should be focus of further investigations.

Magnesium is not only important for bacterial homeostasis but has also been found to inhibit induced autolysis in *E.coli* upon its addition (43). One mutant with a disruption of *mltD* produced low biofilm in this screen. The membrane-bound lytic murein transglycosylase D precursor (*mltD*) encodes for a murein degrading enzyme (autolysin) and belongs to the class of lytic transglycosylases which are important for cell division, insertion of proteins in the cell envelope and also for maintenance of bacterial morphology (44). Lytic transglycosylase activity on cell turnover has previously been linked to increased biofilm formation in Gram-negative (45, 46) and Gram-positive bacteria (47). Cells in a biofilm are protected from exposure to exogenous toxic substances by the surrounding extracellular polymeric substance matrix within a heterogeneous metabolic bacterial population. By altering the cell structure, adhesion to surfaces and ability of matrix production and anchoring is changed (48). Lamers, et al. (49) showed that *mltD* mutants produced about 70% less biofilm than the wild-type *P. aeruginosa*. Similar results were observed by Sailer, et al. (46) for *mltE* mutants of *E. coli*. In our study, *mtlD* mutants could possibly have suffered from interference with components of cell membrane, possibly affecting the surface attachment, important for initial steps of biofilm formation. However, we did not investigate the signaling pathway. It has been shown that a double mutation in two lytic transglycosylases, *mltE* and *mltC*, were specifically linked to the regulation of biofilm formation by affecting the expression of the key biofilm gene regulator CsgD (45) in *S. typhimurium*. Another possible mechanism was proposed by Artola-Recolons, et al. (50). The model involves the maturation of the surrounding peptidoglycan, via lytic transglycosylase, for

345 the proper anchoring and functionality of the flagellar motor, which is required to allow
346 successful colonization of the gastric mucosa by *H. pylori*.

347 In line with a previous finding (51), the *mltD* mutant produced elongated cells when assessed
348 microscopically. The *mltD* mutant (39G5) was one of the few in the screen that exhibited no
349 motility, which is in agreement with other studies (26, 27). Two other low biofilm formers with
350 insertions in the *flaA* gene and a gene encoding for an unknown protein (44F5) were also
351 motility deficient (Figure S6), which might account for their low biofilm production. The
352 successful complementation of the *mltD* mutant, confirmed the gene's direct involvement in
353 biofilm formation and motility. The reduction in motility and production of long chains with
354 elongated cells might impair the ability of the mutant to move freely and to attach to surfaces,
355 thus resulting in biofilm reduction. The observed lower autolysis rate after exposure of 39G5 to
356 Triton X-100 was also seen in a previous study (51) further confirming the involvement of the
357 the *mltD* gene in autolysis.

358 Interestingly, the two genes influenced by magnesium in this study (*mgtB* and *mltD*) are both
359 situated in very close proximity on the genome only 1282 base pairs apart (Supplementary
360 Figure S3b). The coding region for *mltD* is situated on the positive strand and for *mgtB* on the
361 negative strand. A gene encoding for a transcriptional regulator of the TetR family is situated
362 between these two genes. *mltD* is suggested to be regulated by this gene (52), and TetR is
363 known to be influenced by magnesium (53-55). The *mgtB* mutant (44D3) showed a low biofilm
364 phenotype which was reversed to the wild-type level upon magnesium addition, whereas the
365 *mltD* mutant (39G5) showed a further reduction in biofilm mass upon magnesium addition. This
366 and the close proximity of the genes suggest a potential common regulative mechanism,
367 possibly through TetR, although different regulative systems for the two genes have been
368 suggested (35, 52), however, this needs to be further investigated.

This screen also identified a number of mutants with defects in cell wall and membrane functions that showed changes in biofilm formation. Of particular note, a transposon insertion in the *clsA* gene (34F11), encoding for the cardiolipin synthetase, led to enhanced biofilm formation in the present study. Cardiolipin synthetase catalyses the formation of cardiolipin from phosphatidylglycerol and is predominantly active in stationary phase (56). Previous research showed that gene disruption of *clsA* resulted in decreased biofilm formation in other Gram-negative and Gram-positive species (23-25), which indicates that *clsA* might be differentially regulated in different species, possibly due to differences in membrane composition. The hypothesis of differential regulation in multiple species is supported by studies which showed that changes in the environmental conditions, such as osmotic stress or desiccation, led to activation of *clsA* in *E. coli* and *Staphylococcus aureus* (57, 58), but butanol stress induced downregulation of *clsA* in *Bacillus subtilis* (59). By screening a mutant library of *L. monocytogenes* for desiccation survival, Hingston, et al. (16) found that a transposon insertion in the gene encoding for *clsA* resulted in decreased desiccation survival compared to the wild-type in *L. monocytogenes*.

Changes in environmental conditions not only trigger activation of genes involved in membrane composition to protect cells from damage but also trigger other stress response mechanisms. Many studies have shown that stress response is somehow linked to biofilm formation (11, 60-65). One well-described system is the SOS response which is induced upon replication fork stalling caused by DNA damage through reactive oxygen species (ROS) (66). UvrB is part of an enzyme complex that mediates excision and incision steps of DNA repair and its expression is induced as part of the SOS response (67). In this study, a gene disruption of *uvrB* resulted in a low biofilm phenotype, although this phenotype could only be partially complemented. Partial complementation of *uvrB* may have occurred because this gene is part of an operon with *uvrA*, which may also have been affected by the transposon insertion (Figure S3b). The SOS-

response has been linked to biofilm formation in several bacterial species including *L. monocytogenes*, *Pseudomonas aeruginosa* and *Streptococcus mutans* (66-68). Gene expression of *uvrB* and stress response associated genes were found to be upregulated in planktonic cells after heat exposure (69). Microscopic analysis of 33E11 showed changes in phenotype and produced coccoid-shaped bacteria (Figure 3 f). The formation of coccoid-shaped bacteria has been reported previously for *Listeria* cells after exposure to stresses such as starvation due to change from log-growth to long-term survival (70, 71). Tremoulet, et al. (72) found that the bacterial cells of 7-day-old biofilms of *L. monocytogenes* were more coccoid-shaped than rod-shaped, which agrees with our findings. The changes in phenotype might be due to maturation of the biofilm as they did not observe this phenotype for biofilm grown for 24 h.

Although complementation was unsuccessful for the *clsA* and *mgtB* mutants in this study, their repeated identification in the screen, the different locations of the transposon insertions in these mutants and in one instance the different orientation of the transposon (*clsA*) (Table 2) provided substantial evidence for their involvement in biofilm formation.

In addition, both *mgtB* mutants (30H2 and 44D3, Table 2) identified in this screen behaved similarly in the biofilm formation assay, in growth studies (Figure S1 and Table S1) and in motility tests (Figure S6). The two *clsA* mutants (30A9 and 34F11) produced the same amount of biofilm and were also similar in growth behaviour, however, they differed in their motility. The higher motility for one of the *clsA* mutants (30A9) could be due to insertion locations producing a partially functional gene (30A9 – insertion after 1133rd bp as opposed to 729th bp in 34F11). However, this will need further investigation.

Furthermore, the membrane protein cardiolipin is predominantly found at the cell poles of rod-shaped bacteria (73) and lack of cardiolipin might affect incorporation or attachment of specific proteins, such as flagella, into the cell poles resulting in decreased motility. A previous study

found that the swimming motility of *Rhodobacter sphaeroides* was not affected by cardiolipin deficiency (23). However, in contrast to *L. monocytogenes*, which has 4-6 peritrichous flagella, *R. sphaeroides* has just one single flagellum and is usually not situated at the cell pole but medially on the cell body (74). This strengthens the evidence for the involvement of *clsA* in motility and perhaps indicates this only applies to peritrichous flagella.

The inability to restore the wild-type phenotypes in the *mgtB* and *clsA* mutants may have resulted from differential expression of the genes upon site-specific integration of the pIMK vector. This failure may also have been because of polar effects on expression of downstream genes upon insertion of the transposon (Supplementary Figure S3b). Certainly, the orientation of the transposon in the *mgtB* mutant would suggest that the transposon could influence expression of downstream genes such as *ftsW*, which are part of a cell division operon. However, together with literature linking these genes to biofilm formation in other studies (23, 38), their repeated identification provided strong evidence that they are somehow involved in biofilm formation of *L. monocytogenes* 15G01.A recent publication also found an interesting link between cardiolipin and MgtA (which belongs to the same transporter class as MgtB) in *E. coli*: both MgtA and cardiolipin were found together in the bacterial membrane. Subramani, et al. (75) suggested that the head group of cardiolipin contributes to MgtA activation by possibly acting as a chaperone for MgtA. Whether a similar link is present in Gram-positive bacteria will need further investigation.

To conclude, two genes, *clsA* and *mgtB*, were identified to be involved in biofilm formation. Both have, to the best of our knowledge, not previously been associated with biofilm formation in *L. monocytogenes*. The stress responsive gene *uvrB* is clearly part of an operon involved in biofilm formation, strengthening the link between biofilm formation and stress response. Confocal analysis revealed a unique biofilm structure for the *mgtB* mutant, which was reversed upon magnesium addition. Further studies analysing gene regulation are required to assess the exact

involvement of the biofilm-associated genes. Ultimately, this level of understanding could then help devise specific intervention technologies that reduce the tendency of these damaging food-borne pathogens to form such persistent biofilms.

Materials and methods

Bacterial strains and growth conditions

The wild-type strain used in this study was *L. monocytogenes* 15G01, a representative of the persistent pulsotype 5132 obtained from a New Zealand seafood-processing facility during an extensive sampling programme (18). *L. monocytogenes* 15G01 was kept as glycerol stocks in a -80°C freezer and recovered in a three-step process by first growing in Tryptic Soy Broth (TSB) enriched with 0.6% yeast extract (TSBYE) (Difco, BD, USA) overnight at 37°C, then secondly plating on Tryptic Soy Agar enriched with 0.6% yeast extract (TSAYE) (Difco, BD, USA) and, lastly, subculturing and storing on Columbian sheep blood agar (Fort Richard, New Zealand) at 4°C. A library of 6,500 mutants of *L. monocytogenes* 15G01, created by The New Zealand Plant and Food Research Limited using the Himar1 mariner-based transposition system (22) according to a method described previously (76), was kept on 96-well master plates in glycerol at -80°C, subcultured twice before use and stored on TSAYE plates supplemented with erythromycin (Duchefa, Biochemie, The Netherlands) at a final concentration of 5 ppm. Media and agar plates were supplemented with erythromycin at a final concentration of 5 ppm for the studies with the mutants (the transposon contains the erythromycin resistance gene) and with additional kanamycin (MP Biomedicals, Illkirch, France) at a concentration of 50 ppm for the complemented strains. The optical density measurements for the growth studies were taken at a wavelength of 595 or 600 nm using a microplate reader (Multiskan EX, ThermoFisher) or an automated microplate reader (SPECTROstar Omega, BMG Labtech).

Biofilm formation assay

A biofilm formation assay was performed according to the method described by Djordjevic, et al. (77) with some modifications. Briefly, overnight cultures were grown at 37°C in TSBYE in a sterile 96-well plate (polystyrene, U-bottom, Interlab, New Zealand) and transferred to new 96-well plates with a 96-well replicator, each well containing 200 µL modified Welshimer's broth (MWB) (Himedia, India). The cultures were incubated for 48 h at 30°C and then washed three times with 200 µL double-distilled H_2O (ddH_2O) using a microplate strip washer (ELx50, Biotek). After air-drying at ambient temperature for 30 min, 150 µL of a 1% aqueous crystal violet (CV) solution was added to the plates. After 45 min of incubation at 30°C, the CV solution was removed and the cultures were washed six times with 150 µL ddH_2O. After drying for 30 min at 30°C, 150 µL of 96% ethanol was added to each well to de-stain the CV stained cells. The optical density was measured after 1 h at 595 nm with a microplate reader (Multiskan EX, Thermo Fisher). The OD_{595nm} values obtained were corrected by subtracting the OD_{595nm} value of sterile media. To screen the library of transposon mutants, mutants were stored in 96-well master-plates and subcultured twice before tests for biofilm formation. Biofilm formation for each mutant was measured three times and compared to the wild-type strain. Statistical analysis (two sample t-test; $p \leq 0.05$) was performed to select mutants of interest. The OD_{595nm} values of the mutants selected for further analysis were at least 2 standard deviations (SD) above or below that of the wild-type strain. To eliminate variability caused by growth deficiency, biofilm formation and turbidity measurements were repeated for 120 selected mutants in two independent experiments with eight replicates each. Turbidity was measured at 595 nm with a microplate reader before the washing and staining process. The growth of the mutants was compared to the growth of the wild-type in MWB to confirm that the altered biofilm formation observed in the initial screen was not due to differences in the ability of the mutants to grow in this media (Table S1 and Figure S1).

To assess the influence of magnesium on biofilm formation, the CV-assay was carried out in MWB with a final Mg^{2+} concentration of 1.67 mM or 5 mM, respectively. Biofilm formation was measured at 30°C and 37°C for 48 h.

Identification of transposon insertion sites in selected mutants

To locate the transposon insertion sites in the genomes of the mutants of interest, a nested arbitrary PCR was performed using one transposon specific primer and one arbitrary primer (Table 4) to amplify the regions flanking the transposon from the right and the left end. The PCR was performed in two steps with the Mastercycler gradient (Eppendorf, Germany). BioMix Red (Bioline, UK) was used as the mastermix in the first round and the second round was run using AccuPrime Hifi Taq polymerase (Invitrogen, US) as described previously (22). The annealing temperature was adjusted for each mutant if necessary to minimise non-specific annealing or to increase annealing. A final concentration of 3 mM Mg^{2+} was used for all PCR reactions. Five microlitres of each amplified product was visualised on a 1.5% agarose gel (settings 100 V for 30 min) using Redsafe (Intron Biotechnology, Korea) under UV light. The PCR products obtained were subsequently purified and sequenced by Macrogen Ltd. (South Korea) and analysed using the NCBI BLAST programme version 2.2.30 (available from https://www.ncbi.nlm.nih.gov) and the Geneious® 7 programme (available from http://www.geneious.com) (78). The reference strain *L. monocytogenes* EGD (accession HG421741) (79) was used to identify the coordinates at the point of the transposon insertion site and the orientation of the transposon in the chromosome. This reference strain was chosen as it is the same serotype as the *L. monocytogenes* 15G01 strain (1/2a).

Complementation of selected mutants

The site-specific integrative vector pIMK (80) was used for the genetic complementation of selected mutants. The vector pIMK is a derivative of pPL2 (1Kb smaller) and facilitates the

519 insertion at the $tRNA_{Arg}$ locus (81). Genetic complementation constructs using this plasmid were
520 constructed by amplifying the target genes from wild-type 15G01 using gene-specific primers in
521 PCR (Table 4). The gene-specific PCR products and the pIMK vector were digested with *Pst*I
522 and *Bam*HI and ligated to one another using the LigaFast™ Rapid DNA Ligation System
523 (Promega, USA), following the manufacturer's instructions, in a molar ratio 3:1 (vector to insert).
524 One microlitre of the recombinant plasmid was then introduced into chemically competent
525 *Escherichia coli* S17 cells by heat shock. Transformants were selected on Luria Bertani (LB)
526 agar plates supplemented with kanamycin. A colony was picked from the agar plate with a
527 sterile toothpick and dipped in the PCR-mix. Colony PCR was performed with one gene-specific
528 primer and T7 (T7 binding site present in the pIMK plasmid) to confirm successful
529 transformation. Recombinant plasmids were extracted from colony PCR-positive cultures and
530 the gene inserts were sequenced to confirm the authenticity of the constructs. Authentic
531 transformants were then used for the genetic complementation of *L. monocytogenes* 15G01
532 mutants. Conjugation was performed according to Azizoglu, et al. (82) with some modifications.
533 Single colonies of the donor (*E. coli* transformants containing the construct pIMK:gene or a
534 control containing only the pIMK vector) were resuspended overnight in LB broth containing
535 kanamycin and incubated at 30°C, at 100 rpm to an OD_{595nm} of approximately 0.55. At the same
536 time, a colony of the recipient (*L. monocytogenes* 15G01 transposon mutant) was resuspended
537 in Brain-Heart-Infusion (BHI) (Difco, BD, USA) medium and incubated overnight at 37°C with
538 shaking. The donor culture (3 mL) and a pre-warmed (45°C; 10 min) recipient culture (1.5 mL)
539 were mixed together and centrifuged at 2050 g for 8 min; the bacterial pellet was then washed
540 with 10 mL of BHI broth and centrifuged again using the same conditions. After washing, the
541 pellet was resuspended in 500 µL of fresh BHI broth, deposited in the centre of a BHI agar plate
542 and incubated overnight at 37°C. The drop was then resuspended in 2 mL BHI broth and a 100
543 µL aliquot was spread-plated on BHI agar plates containing kanamycin and nalidixic acid (Fort
544 Richard, New Zealand) (20 µg/mL). *L. monocytogenes* strains are naturally resistant against

545 nalidixic acid and therefore it was used for counterselection. The plates were incubated at 30°C
546 for 2-3 days. The authenticity of transconjugants was confirmed by colony PCR using the
547 corresponding gene-specific primers. Their identity as *L. monocytogenes* was also confirmed
548 using 16S-rRNA specific primers for *L. monocytogenes* (Table 4). To confirm that the empty
549 vector had no effect on the phenotype, the parent plasmid was transformed in each mutant as
550 well as the wild-type strain 15G01.

551 **Microscopic analysis**

552 Fluorescence microscopy, scanning electron microscopy (SEM) and confocal laser scanning
553 microscopy were used to visualise biofilm formation of bacterial strains on polystyrene, stainless
554 steel and glass, respectively. For visualisation under fluorescence, the fluorescent LIVE/DEAD
555 *Bac*Light bacterial viability kit (Life Technologies, Thermo Fisher, New Zealand) was used to
556 label living cells green (SYTO9, membrane-permeable stain) and dead cells red (propidium
557 iodide, a non-membrane permeable stain). Six-well plates (tissue treated, Greiner, Germany)
558 were filled with 2.97 mL MWB and inoculated with 30 µL of an overnight bacterial culture grown
559 in TSBYE at 37°C and were incubated at 30°C for 48 h. The biofilms were then washed twice
560 with 0.8% NaCl to remove loosely attached cells and stained with 1 mL fluorescent stain
561 prepared according to the manufacturer's manual. A fluorescence microscope (Olympus, BX51
562 fitted with the XC30 digital camera) was used at 10 x 100 magnification to take images.

563 SEM was performed on stainless steel coupons (5x5 mm, food grade) as described previously
564 (83). The coupons were coated with cooked mussel juice (CMJ) produced as described
565 previously (19), but with some modifications. Briefly, Greenshell™ mussels obtained from the
566 local supermarket were stored for 24 h at 10°C in a fridge and then boiled in a wok closed with a
567 lid without addition of water. When all mussels opened and released the intervalvular juice, the
568 liquid was collected and autoclaved at 121°C for 15 min. The coupons were pre-treated with
569 alkali detergent for 2 h at 45°C and then rinsed with ddH_20 and autoclaved in deionised water.

570 The coupons were coated by immersion in CMJ in a 6-well plate (tissue treated, Greiner,
571 Germany) for 4 h at 60°C (or until dried). The coupons were then placed into a fresh 6-well plate
572 containing MWB (2.97 mL) and were inoculated with 30 µL of an overnight culture of the
573 bacterium ($10^{7.5}$–10^{8} CFU). After incubation for 7 d at 30°C, phosphate buffered saline (PBS)
574 (pH 7.2) was used to remove loosely attached cells on the coupons. After rinsing with 100 mM
575 cacodylate buffer (pH 7.2) (Acros Organics, NJ, USA) the coupons were fixed overnight at 4°C
576 in 2 % glutaraldehyde (Acros Organics, NJ, USA) and 0.1 % ruthenium red solution (Acros
577 Organics, NJ, USA) in 100 mM cacodylate buffer. The next morning, coupons were rinsed to
578 remove unbound dye and then dehydrated in serial dilutions of ethanol for 10 min each (30, 50,
579 60, 70, 90 % v/v) with three final 10 min rinses in absolute ethanol. The coupons were then
580 critical point dried (BalTec CPD030 (BalTec AG, Balzers, Liechtenstein)) and sputter coated
581 with gold (Leica EM ACE200, (Leica Microscopy Systems Ltd, Heerbrugg, Switzerland)) for
582 visualisation using a scanning electron microscope (FEI Quanta 250 SEM (Fei Company,
583 Hillsboro, OR)).

584 For confocal laser scanning microscopy (CLSM) analysis, the biofilms were grown on glass-
585 bottom dishes (35mm petri dish, 10mm Microwell No. 0 coverglass, MatTek Corporation, USA).
586 First, single colonies picked from an agar plate (TSAYE) were used to inoculate TSBYE and
587 then incubated overnight at 37°C. The glass-bottom dishes were filled with 2.97 mL MWB (Mg^{2+}
588 concentration 1.67 mM or 5 mM) and inoculated with 30 µL of the overnight culture. After 7 d
589 incubation at 30°C (or 37°C for 39G5), the medium was carefully removed and the biofilm on the
590 plates washed twice with 0.8% NaCl solution. The fluorescent LIVE/DEAD *Bac*Light bacterial
591 viability kit was used to stain the biofilms according to the manufacturer's instructions. Three
592 images (246.03x246.03 µm) per sample were taken with a Leica DM6000B scanning confocal
593 microscope running LAS AF software version 2.7.3.9723. Excitation and emission were as

follows: Stains: SYTO9, excitation @ 488 nm (argon laser), emission collection @ 498–550 nm; propidium iodide, excitation @ 561 nm (DPSS 561 laser), emission collection @ 571–700 nm. Images were analysed using ImageJ software and/or Imaris (Bitplane, Zurich). COMSTAT (available from www.comstat.dk) was used to calculate biomass, roughness, maximum and average thickness of the biofilms (84, 85).

Motility assay

A motility assay was performed according to the method of Knudsen, et al. (86). Briefly, semi-solid agar plates (TSB+0.25% Agar (Difco, BD, USA)) were inoculated with *L. monocytogenes* 15G01 or the mutant (39G5) using a sterile pick and incubated at 30°C or 37°C for 48 h. The diameter of the halo formed around the colony was then measured and compared to halo surrounding the wild-type strain (15G01). Three independent experiments were performed with each treatment repeated in triplicate.

Autolysis assay

The assay was performed according to Huang, et al. (10) with minor modifications. Briefly, single colonies of the wild-type and the selected mutant (39G5) were picked from the TSAYE plate and grown in BHI at 37°C overnight. OD_{595nm} was measured in a microplate reader (SPECTROstar Omega, BMG Labtech) and adjusted to 0.6 ± 0.05 for each culture. Each culture (1.5 mL) was transferred to 2 mL microtubes and centrifuged at 4°C at 4500 g for 10 min. The supernatant was discarded, and the cell pellet washed twice with ice cold ddH_2O, then resuspended in the same volume of Tris-HCl (pH 7.2) containing 0.05% Triton-X-100. Solutions with cells were incubated at 30°C in a 96-well plate and the OD_{595nm} was measured for 20 h in 5 min intervals using an automated microplate reader (SPECTROstar Omega, BMG Labtech).

Acknowledgements

The authors would like to thank Erik Rikkerink and Falk Kalamorz for their valuable feedback on the manuscript, Duncan Hedderley for the help with the statistical analysis and Ian Hallett and Paul Sutherland for their help with the SEM. This research was funded through The New Zealand Ministry of Business, Innovation and Employment (MBIE) funding: contract CAWX1801.

Authors declare that there are no conflicts of interest, and that the research does not involve human participants and / or animals.

Data Availability Statement

The data that support the findings of this study are available from the corresponding author upon reasonable request.

References

1. Rocourt J, Jacquet C, Reilly A. 2000. Epidemiology of human listeriosis and seafoods. Int J Food Microbiol. **62:**197-209.
2. Lecuit M. 2005. Understanding how Listeria monocytogenes targets and crosses host barriers. Clin Microbiol Infect. **11:**430-436.
3. Fletcher G, Rogers M, Wong R. 1994. Survey of Listeria monocytogenes in New Zealand seafood. J Aquat Food Prod T. **3:**13-24.
4. Gudbjörnsdóttir B, Suihko ML, Gustavsson P, Thorkelsson G, Salo S, Sjöberg AM, Niclasen O, Bredholt S. 2004. The incidence of Listeria monocytogenes in meat, poultry and seafood plants in the Nordic countries. Food Microbiol. **21:**217-225.
5. Srey S, Jahid IK, Ha S-D. 2013. Biofilm formation in food industries: A food safety concern. Food Control. **31:**572-585.
6. Yousef AE. 1999. Characteristics of *Listeria monocytogenes* important to food processors. Listeria Listeriosis Food Safety**:**131.
7. Carpentier B, Cerf O. 2011. Review--Persistence of Listeria monocytogenes in food industry equipment and premises. Int J Food Microbiol. **145:**1-8.
8. Cruz CD, Fletcher GC. 2012. Assessing manufacturers' recommended concentrations of commercial sanitizers on inactivation of Listeria monocytogenes. Food Control. **26:**194-199.
9. Van Houdt R, Michiels CW. 2010. Biofilm formation and the food industry, a focus on the bacterial outer surface. J Appl Microbiol. **109:**1117-1131.
10. Huang Y, Shi C, Yu S, Li K, Shi X. 2012. A putative MerR family regulator involved in biofilm formation in Listeria monocytogenes 4b G. Foodborne Pathog Dis. **9:**767-772.
11. Huang Y, Suo Y, Shi C, Szlavik J, Shi XM, Knochel S. 2013. Mutations in gltB and gltC reduce oxidative stress tolerance and biofilm formation in Listeria monocytogenes 4b G. Int J Food Microbiol. **163:**223-230.
12. Alonso AN, Perry KJ, Regeimbal JM, Regan PM, Higgins DE. 2014. Identification of Listeria monocytogenes Determinants Required for Biofilm Formation. PLoS ONE. **9:**e113696.
13. Chang Y, Gu W, Fischer N, McLandsborough L. 2012. Identification of genes involved in Listeria monocytogenes biofilm formation by mariner-based transposon mutagenesis. Appl Microbiol Biotechnol. **93:**2051-2062.
14. Ouyang Y, Li J, Dong Y, Blakely LV, Cao M. 2012. Genome-wide screening of genes required for Listeria monocytogenes biofilm formation. J Biotech Res. **4:**13-25.
15. Piercey MJ, Hingston PA, Truelstrup Hansen L. 2016. Genes involved in Listeria monocytogenes biofilm formation at a simulated food processing plant temperature of 15 degrees C. Int J Food Microbiol. **223:**63-74.
16. Hingston PA, Piercey MJ, Truelstrup Hansen L. 2015. Genes Associated with Desiccation and Osmotic Stress in Listeria monocytogenes as Revealed by Insertional Mutagenesis. Appl Environ Microbiol. **81:**5350-5362.
17. Collins B, Joyce S, Hill C, Cotter PD, Ross RP. 2010. TelA contributes to the innate resistance of Listeria monocytogenes to nisin and other cell wall-acting antibiotics. Antimicrob Agents Chemother. **54:**4658-4663.
18. Cruz CD, Fletcher GC. 2011. Prevalence and biofilm-forming ability of Listeria monocytogenes in New Zealand mussel (Perna canaliculus) processing plants. Food Microbiol. **28:**1387-1393.
19. Nowak J, Cruz CD, Palmer J, Fletcher GC, Flint S. 2015. Biofilm formation of the *L. monocytogenes* strain 15G01 is influenced by changes in environmental conditions. J Microbiol Methods. **119:**189-195.

679 20. Nowak J, Cruz CD, Tempelaars M, Abee T, van Vliet AHM, Fletcher GC, Hedderley D, Palmer J, Flint S.
680 2017. Persistent Listeria monocytogenes strains isolated from mussel production facilities form
681 more biofilm but are not linked to specific genetic markers. Int J Food Microbiol. **256:**45-53.
682 21. Cruz CD, Pitman AR, Harrow SA, Fletcher GC. 2014. Listeria monocytogenes associated with New
683 Zealand seafood production and clinical cases: unique sequence types, truncated InlA, and
684 attenuated invasiveness. Appl. Environ. Microbiol. **80:**1489-1497.
685 22. Nowak J, Visnovsky S, Cruz CD, Fletcher G, van Vliet AHM, Hedderley D, Butler R, Flint S, Palmer J,
686 Pitman A. Inactivation of the gene encoding the cationic antimicrobial peptide resistance factor
687 MprF increases biofilm formation but reduces invasiveness of Listeria monocytogenes. J. Appl.
688 Microbiol. **n/a**.
689 23. Lin TY, Santos TM, Kontur WS, Donohue TJ, Weibel DB. 2015. A Cardiolipin-Deficient Mutant of
690 Rhodobacter sphaeroides Has an Altered Cell Shape and Is Impaired in Biofilm Formation. J
691 Bacteriol. **197:**3446-3455.
692 24. Munoz-Elias EJ, Marcano J, Camilli A. 2008. Isolation of Streptococcus pneumoniae biofilm mutants
693 and their characterization during nasopharyngeal colonization. Infect Immun. **76:**5049-5061.
694 25. Puttamreddy S, Cornick NA, Minion FC. 2010. Genome-wide transposon mutagenesis reveals a role
695 for pO157 genes in biofilm development in Escherichia coli O157:H7 EDL933. Infect Immun.
696 **78:**2377-2384.
697 26. Machata S, Hain T, Rohde M, Chakraborty T. 2005. Simultaneous deficiency of both MurA and p60
698 proteins generates a rough phenotype in Listeria monocytogenes. J Bacteriol. **187:**8385-8394.
699 27. Machata S. 2008. Molecular investigations of peptidoglycanbinding proteins in Listeria
700 monocytogenes PhD. Justus-Liebig-Universitaet Giessen, Giessen.
701 28. Bao Y, Zhang X, Jiang Q, Xue T, Sun B. 2015. Pfs promotes autolysis-dependent release of eDNA and
702 biofilm formation in Staphylococcus aureus. Med Microbiol Immunol. **204:**215-226.
703 29. Webb AJ, Karatsa-Dodgson M, Grundling A. 2009. Two-enzyme systems for glycolipid and
704 polyglycerolphosphate lipoteichoic acid synthesis in Listeria monocytogenes. Mol Microbiol.
705 **74:**299-314.
706 30. Parsek MR, Fuqua C. 2004. Biofilms 2003: emerging themes and challenges in studies of surface-
707 associated microbial life. J Bacteriol. **186:**4427-4440.
708 31. Mulcahy H, Lewenza S. 2011. Magnesium limitation is an environmental trigger of the Pseudomonas
709 aeruginosa biofilm lifestyle. PLoS ONE. **6:**e23307.
710 32. Kehres DG, Maguire ME. 2003. The Unusual Nature of Magnesium Transporters, p. 347-360,
711 Microbial Transport Systems. Wiley-VCH Verlag GmbH & Co. KGaA.
712 33. Chamnongpol S, Groisman EA. 2002. Mg2+ homeostasis and avoidance of metal toxicity. Mol
713 Microbiol. **44:**561-571.
714 34. Groisman EA, Cromie MJ, Shi Y, Latifi T. 2006. A Mg2+-responding RNA that controls the expression
715 of a Mg2+ transporter. Cold Spring Harb Symp Quant Biol. **71:**251-258.
716 35. Nielsen PK, Andersen AZ, Mols M, van der Veen S, Abee T, Kallipolitis BH. 2012. Genome-wide
717 transcriptional profiling of the cell envelope stress response and the role of LisRK and CesRK in
718 Listeria monocytogenes. Microbiol. **158:**963-974.
719 36. Kallipolitis BH, Ingmer H, Gahan CG, Hill C, Søgaard-Andersen L. 2003. CesRK, a Two-Component
720 Signal Transduction System in *Listeria monocytogenes*, Responds to the Presence of Cell Wall-
721 Acting Antibiotics and Affects β-Lactam Resistance. Antimicrob. Agents Chemother. **47:**3421-
722 3429.
723 37. Gottschalk S, Bygebjerg-Hove I, Bonde M, Nielsen PK, Nguyen TH, Gravesen A, Kallipolitis BH. 2008.
724 The two-component system CesRK controls the transcriptional induction of cell envelope-
725 related genes in Listeria monocytogenes in response to cell wall-acting antibiotics. J Bacteriol.
726 **190:**4772-4776.

38. Hartmann I, Carranza P, Lehner A, Stephan R, Eberl L, Riedel K. 2010. Genes Involved in Cronobacter sakazakii Biofilm Formation. Appl. Environ. Microbiol. **76:**2251-2261.
39. Coffey BM, Akhand SS, Anderson GG. 2014. MgtE is a dual-function protein in Pseudomonas aeruginosa. Microbiol. **160:**1200-1213.
40. Guilbaud M, Piveteau P, Desvaux M, Brisse S, Briandet R. 2015. Exploring the diversity of Listeria monocytogenes biofilm architecture by high-throughput confocal laser scanning microscopy and the predominance of the honeycomb-like morphotype. Appl Environ Microbiol. **81:**1813-1819.
41. Oknin H, Steinberg D, Shemesh M. 2015. Magnesium ions mitigate biofilm formation of Bacillus species via downregulation of matrix genes expression. Frontiers in microbiology. **6:**907.
42. Song B, Leff LG. 2006. Influence of magnesium ions on biofilm formation by Pseudomonas fluorescens. Microbiol. Res. **161:**355-361.
43. Leduc M, Kasra R, van Heijenoort J. 1982. Induction and control of the autolytic system of Escherichia coli. J Bacteriol. **152:**26-34.
44. Scheurwater E, Reid CW, Clarke AJ. 2008. Lytic transglycosylases: bacterial space-making autolysins. Int J Biochem Cell Biol. **40:**586-591.
45. Monteiro C, Fang X, Ahmad I, Gomelsky M, Römling U. 2011. Regulation of biofilm components in Salmonella enterica serovar Typhimurium by lytic transglycosylases involved in cell wall turnover. J. Bacteriol. **193:**6443-6451.
46. Sailer FC, Meberg BM, Young KD. 2003. β-Lactam induction of colanic acid gene expression in Escherichia coli. FEMS Microbiol. Lett. **226:**245-249.
47. Kolar SL, Nagarajan V, Oszmiana A, Rivera FE, Miller HK, Davenport JE, Riordan JT, Potempa J, Barber DS, Koziel J. 2011. NsaRS is a cell-envelope-stress-sensing two-component system of Staphylococcus aureus. Microbiol. **157:**2206.
48. Bucher T, Oppenheimer‐Shaanan Y, Savidor A, Bloom‐Ackermann Z, Kolodkin‐Gal I. 2015. Disturbance of the bacterial cell wall specifically interferes with biofilm formation. Environmental microbiology reports. **7:**990-1004.
49. Lamers RP, Nguyen UT, Nguyen Y, Buensuceso RN, Burrows LL. 2015. Loss of membrane‐bound lytic transglycosylases increases outer membrane permeability and β‐lactam sensitivity in Pseudomonas aeruginosa. Microbiologyopen. **4:**879-895.
50. Artola-Recolons C, Lee M, Bernardo-García N, Blázquez B, Hesek D, Bartual SG, Mahasenan KV, Lastochkin E, Pi H, Boggess B. 2014. Structure and cell wall cleavage by modular lytic transglycosylase MltC of Escherichia coli. ACS chemical biology. **9:**2058-2066.
51. Carroll SA, Hain T, Technow U, Darji A, Pashalidis P, Joseph SW, Chakraborty T. 2003. Identification and characterization of a peptidoglycan hydrolase, MurA, of Listeria monocytogenes, a muramidase needed for cell separation. J Bacteriol. **185:**6801-6808.
52. Chatterjee SS, Hossain H, Otten S, Kuenne C, Kuchmina K, Machata S, Domann E, Chakraborty T, Hain T. 2006. Intracellular gene expression profile of Listeria monocytogenes. Infect Immun. **74:**1323-1338.
53. Leypold CF, Marian DT, Roman C, Schneider S, Schubert P, Scholz O, Hillen W, Clark T, Lanig H. 2004. How does Mg(2+) affect the binding of anhydrotetracycline in the TetR protein? Photochem Photobiol Sci. **3:**109-119.
54. Scholz O, Schubert P, Kintrup M, Hillen W. 2000. Tet repressor induction without Mg2+. Biochem. **39:**10914-10920.
55. Werten S, Dalm D, Palm GJ, Grimm CC, Hinrichs W. 2014. Tetracycline repressor allostery does not depend on divalent metal recognition. Biochem. **53:**7990-7998.
56. Koprivnjak T, Zhang D, Ernst CM, Peschel A, Nauseef WM, Weiss JP. 2011. Characterization of Staphylococcus aureus cardiolipin synthases 1 and 2 and their contribution to accumulation of cardiolipin in stationary phase and within phagocytes. J Bacteriol. **193:**4134-4142.

57. Maudsdotter L, Imai S, Ohniwa RL, Saito S, Morikawa K. 2015. Staphylococcus aureus dry stress survivors have a heritable fitness advantage in subsequent dry exposure. Microbes Infect. **17:**456-461.
58. Romantsov T, Guan Z, Wood JM. 2009. Cardiolipin and the osmotic stress responses of bacteria. Biochim Biophys Acta. **1788:**2092-2100.
59. Vinayavekhin N, Mahipant G, Vangnai AS, Sangvanich P. 2015. Untargeted metabolomics analysis revealed changes in the composition of glycerolipids and phospholipids in Bacillus subtilis under 1-butanol stress. Appl Microbiol Biotechnol. **99:**5971-5983.
60. Suo Y, Huang Y, Liu Y, Shi C, Shi X. 2012. The expression of superoxide dismutase (SOD) and a putative ABC transporter permease is inversely correlated during biofilm formation in Listeria monocytogenes 4b G. PLoS ONE. **7:**e48467.
61. Taylor CM, Beresford M, Epton HA, Sigee DC, Shama G, Andrew PW, Roberts IS. 2002. Listeria monocytogenes relA and hpt mutants are impaired in surface-attached growth and virulence. J Bacteriol. **184:**621-628.
62. van der Veen S, Abee T. 2010. Dependence of continuous-flow biofilm formation by Listeria monocytogenes EGD-e on SOS response factor YneA. Appl Environ Microbiol. **76:**1992-1995.
63. van der Veen S, Abee T. 2010. HrcA and DnaK are important for static and continuous-flow biofilm formation and disinfectant resistance in Listeria monocytogenes. Microbiol. **156:**3782-3790.
64. van der Veen S, Abee T. 2010. Importance of SigB for Listeria monocytogenes static and continuous-flow biofilm formation and disinfectant resistance. Appl Environ Microbiol. **76:**7854-7860.
65. van der Veen S, Abee T. 2011. Generation of variants in Listeria monocytogenes continuous-flow biofilms is dependent on radical-induced DNA damage and RecA-mediated repair. PLoS ONE. **6:**e28590.
66. van der Veen S, Abee T. 2011. Bacterial SOS response: a food safety perspective. Curr Opin Biotechnol. **22:**136-142.
67. van der Veen S, van Schalkwijk S, Molenaar D, de Vos WM, Abee T, Wells-Bennik MH. 2010. The SOS response of Listeria monocytogenes is involved in stress resistance and mutagenesis. Microbiol. **156:**374-384.
68. Inagaki S, Matsumoto-Nakano M, Fujita K, Nagayama K, Funao J, Ooshima T. 2009. Effects of recombinase A deficiency on biofilm formation by *Streptococcus mutans*. Oral Microbiol Immunol. **24:**104-108.
69. van der Veen S, Hain T, Wouters JA, Hossain H, de Vos WM, Abee T, Chakraborty T, Wells-Bennik MH. 2007. The heat-shock response of Listeria monocytogenes comprises genes involved in heat shock, cell division, cell wall synthesis, and the SOS response. Microbiol. **153:**3593-3607.
70. Doijad SP, Barbuddhe SB, Garg S, Poharkar KV, Kalorey DR, Kurkure NV, Rawool DB, Chakraborty T. 2015. Biofilm-Forming Abilities of Listeria monocytogenes Serotypes Isolated from Different Sources. PLoS ONE. **10:**e0137046.
71. Wen J, Anantheswaran RC, Knabel SJ. 2009. Changes in barotolerance, thermotolerance, and cellular morphology throughout the life cycle of Listeria monocytogenes. Appl Environ Microbiol. **75:**1581-1588.
72. Tremoulet F, Duche O, Namane A, Martinie B, Labadie JC, European Listeria Genome C. 2002. Comparison of protein patterns of Listeria monocytogenes grown in biofilm or in planktonic mode by proteomic analysis. FEMS Microbiol Lett. **210:**25-31.
73. Dworkin J. 2009. Cellular Polarity in Prokaryotic Organisms. Cold Spring Harbor Persp. Biol. **1:**a003368.
74. Armitage JP, Macnab RM. 1987. Unidirectional, intermittent rotation of the flagellum of Rhodobacter sphaeroides. J Bacteriol. **169:**514-518.

75. Subramani S, Perdreau-Dahl H, Morth JP. 2016. The magnesium transporter A is activated by cardiolipin and is highly sensitive to free magnesium in vitro. eLife. **5**.
76. Cao M, Bitar AP, Marquis H. 2007. A mariner-based transposition system for Listeria monocytogenes. Appl Environ Microbiol. **73:**2758-2761.
77. Djordjevic D, Wiedmann M, McLandsborough LA. 2002. Microtiter plate assay for assessment of *Listeria monocytogenes* biofilm formation. Appl Environ Microbiol. **68:**2950-2958.
78. Kearse M, Moir R, Wilson A, Stones-Havas S, Cheung M, Sturrock S, Buxton S, Cooper A, Markowitz S, Duran C, Thierer T, Ashton B, Meintjes P, Drummond A. 2012. Geneious Basic: an integrated and extendable desktop software platform for the organization and analysis of sequence data. Bioinformatics. **28:**1647-1649.
79. Becavin C, Bouchier C, Lechat P, Archambaud C, Creno S, Gouin E, Wu Z, Kuhbacher A, Brisse S, Pucciarelli MG, Garcia-del Portillo F, Hain T, Portnoy DA, Chakraborty T, Lecuit M, Pizarro-Cerda J, Moszer I, Bierne H, Cossart P. 2014. Comparison of widely used Listeria monocytogenes strains EGD, 10403S, and EGD-e highlights genomic variations underlying differences in pathogenicity. mBio. **5:**e00969-00914.
80. Monk IR, Gahan CG, Hill C. 2008. Tools for functional postgenomic analysis of listeria monocytogenes. Appl Environ Microbiol. **74:**3921-3934.
81. Lauer P, Chow MY, Loessner MJ, Portnoy DA, Calendar R. 2002. Construction, characterization, and use of two Listeria monocytogenes site-specific phage integration vectors. J Bacteriol. **184:**4177-4186.
82. Azizoglu RO, Elhanafi D, Kathariou S. 2014. Mutant construction and integration vector-mediated gene complementation in Listeria monocytogenes. Methods Mol Biol. **1157:**201-211.
83. Borucki MK, Peppin JD, White D, Loge F, Call DR. 2003. Variation in biofilm formation among strains of *Listeria monocytogenes*. Appl Environ Microbiol. **69:**7336-7342.
84. Heydorn A, Nielsen AT, Hentzer M, Sternberg C, Givskov M, Ersboll BK, Molin S. 2000. Quantification of biofilm structures by the novel computer program COMSTAT. Microbiol. (Reading). **146 (Pt 10):**2395-2407.
85. Vorregaard M. 2008. Comstat2-a modern 3D image analysis environment for biofilms. Technical University of Denmark
86. Knudsen GM, Olsen JE, Dons L. 2004. Characterization of DegU, a response regulator in *Listeria monocytogenes*, involved in regulation of motility and contributes to virulence. FEMS Microbiol Lett. **240:**171-179.
87. Park S, Jung J, Choi S, Oh Y, Lee J, Chae H, Ryu S, Jung H, Park G, Choi S. 2012. Molecular Characterization of Listeria monocytogenes Based on the PFGE and RAPD in Korea. Adv Microbiol. **2:**ID: 26214.

865

866

867

Tables

Table 1. Bacterial strains and plasmids used in this study

Bacterial strains and plasmids		***Mutation***	***Source***
<u>*Bacterial strains*</u>			
Listeria monocytogenes 15G01	Wild-type serotype 1/2a; Em^S, Kan^S		Cruz and Fletcher (18)
34F11	15G01 with transposon inserted in the *clsA* gene (*LMON_2515)*; Em^R, Kan^S	15G01 *clsA*::himar1	This study
33E11	15G01 with transposon inserted in the *uvrB* gene (*LMON_2501*); Em^R, Kan^S	15G01 *uvrB*::himar1	This study
33E11-C	33E11 containing the pIMK-uvrB plasmid; Em^R, Kan^R	15G01 *uvrB*::himar1/pIMK*uvrB*	This study
33E11-EV	33E11 containing the pIMK plasmid; Em^R, Kan^R	15G01 *uvrB*::himar1/pIMK	This study
39G5	15G01 with transposon inserted in the *mltD* gene (*LMON_2714*); Em^R, Kan^S	15G01 *mltD*::himar1	This study
39G5-C	39G5 containing the pIMK-mltD plasmid; Em^R, Kan^R	15G01 *mltD*::himar1/pIMK*mltD*	This study
39G5-EV	39G5 containing the pIMK plasmid; Em^R, Kan^R	15G01 *mltD*::himar1/pIMK	This study
44D3	15G01 with transposon inserted in the mgtB gene (*LMON_2712*); Em^R, Kan^S	15G01 *mgtB*::himar1	This study
41H7	15G01 with transposon inserted in the *flaA* gene (*LMON_0695*); Em^R, Kan^S	15G01 *flaA*::himar1	This study
<u>*Plasmids*</u>			
pIMK	Site-specific listerial integrative vector, 5.1 kb, Kan^R		Monk, et al. (80)
pIMK-uvrB	Site-specific plasmid carrying the *LMON_2501* gene; Kan^R		This study
pIMK-mltD	Site-specific plasmid carrying the *LMON_2714* gene, Kan^R		This study

871 **Table 2.** Biofilm-related genes identified in *Listeria monocytogenes* 15G01 through transposon insertions based on DNA homologies with *L.*
872 *monocytogenes* EGD genome database, accession HG421741. Homologies were identified by Megablast and Geneious® 7 software using
873 default settings. The biofilm mass produced by the mutants (CV-assay) was calculated relative to the biofilm formation of the wild-type in two
874 independent experiments with eight replicates. Putative gene functions are based on the information from http://www.genome.jp/.

Function group and putative gene function	**Transposon insertion site**	**Biofilm mass relative to wt strain [%] mean ± SD**	**Number of hits**	**Coordinates for insertion in *L. monocytogenes* EGD**	**Orientation of transposon insertion**	**Mutant strain [a]**
Biosynthesis						
Adenylosuccinate synthase	*LMON_0057 (purA)*	135.7 ± 5.12	1	59174	3'-5'	24A10
Dihydroxyacetone kinase family protein	*LMON_1882*	173.03 ± 7.82	1	1888930	3'-5'	35H9
Acetyltransferase, GNAT family	*LMON_2362*	27.32 ± 6.92	1	2377834	5'-3'	31E7
Glycosyl hydrolase, family 31	*LMON_2457*	19.90 ± 4.93	1	[c]	3'-5'	32E5
Cell wall / membrane						
Sortase A, LPXTG specific SrtA	*LMON_0935*	7.49 ± 0.59	1	948604	3'-5'	31C7
Glycosyltransferase	*LMON_0939*	18.74 ± 3.36	1	[c]	5'-3'	35C1
Putative peptidoglycan bound protein (LPXTG motif) Lmo1666 homologue	*LMON_1733*	29.70 ± 5.66	3	1723653, 1721718, 1721318	5'-3', 3'-5', 3'-5'	24H3, 25D2, 64B3
Cardiolipin synthetase ClsA	*LMON_2515*	163.02 ± 15.27	2	2538121, 2538525	3'-5', 5'-3'	30A9, 34F11
Glycosyltransferase LafA	*LMON_2570*	16.10 ± 2.43	2	2591134, 2590370	3'-5', 3'-5'	28G11, 32A9
Translation and Transcription						
GTP-binding protein HflX	*LMON_1358*	16.06 ± 6.92	1	[c]	3'-5'	43C9
SSU ribosomal protein S1p	*LMON_2007 (rpsA)*	140.68 ± 10.74	1	2012734	3'-5'	28A2

Transporter systems						
Manganese ABC transporter, ATP-binding protein SitB	*LMON_1917*	133.83 ± 7.38	1	1925244	3'-5'	47H11
Bacitracin export ATP-binding protein BceA	*LMON_2188*	138.01 ± 1.19	1	2194403	3'-5'	31G1
ABC transporter, permease protein EscB	*LMON_2290*	142.51 ± 7.66	2	2305608, 2305511	3'-5', 3'-5'	32E2, 47H10
Phosphate ABC transporter, periplasmic phosphate-binding protein PstS	*LMON_2511*	30.81 ± 0.50	1	2532962	3'-5'	36A2
PTS system, IIA component	*LMON_2675*	32.69 ± 3.94	1	2692293	3'-5'	26C10
$Mg^{(2+)}$ transport ATPase, P-type	*LMON_2712*	7.16 ± 1.47	2	2731046, 2731895	3'-5', 3'-5'	30H2, 44D3
ABC transporter, ATP-binding protein	*LMON_2792*	6.93 ± 0.27	1	2816670	3'-5'	28D10
Motility						
Flagellin protein FlaA	*LMON_0695 (flaA)*	23.74 ± 5.93	1	[c]	3'-5'	41H7
Autolysis						
Membrane-bound lytic murein transglycosylase D precursor MltD	*LMON_2714*	2.11 ± 0.35	1	2734305	5'-3'	39G5
DNA repair and stress response						
Glutamate decarboxylase	*LMON_2376*	6.81 ± 0.93	1	2393310	3'-5'	35F3
Excinuclease ABC subunit B UvrB	*LMON_2501 (uvrB)*	18.33 ± 2.58	2	2525427, 2525564	3'-5', 3'-5'	33E11, 42G3
Unknown						
FIG00774663: hypothetical protein	*LMON_1212*	21.32 ± 0.69	1	[c]	5'-3'	36B9
FIG00774466: hypothetical protein	*LMON_2144*	28.89 ± 3.37	1	2153693	5'-3'	26H1
COG1801: Uncharacterized conserved protein	*LMON_2417*	15.37 ± 0.51	1	[c]	3'-5'	40C12
Hypothetical protein (mutant strain 44F5)	[b]	10.70 ± 5.02	1	[c]	3'-5'	44F5

Hypothetical protein (mutant strain 41A8)	[b]	21.88 ± 7.19	1	[c]	3'-5'	41A8
Intergenic[d]						
Methionine ABC transporter ATP-binding protein and hypothetical protein	*LMON_2430 & LMON_2431*	18.27 ± 1.96	1	2450096	3'-5'	67C5
Dihydroxyacetone kinase family protein and putative alkaline-shock protein	*LMON_1882 & LMON_1883*	173.44 ± 15.52	1	1889436	3'-5'	33F8

[a] Internal numbering of the transposon library
[b] No counterpart in *L. monocytogenes* EGD, but present in parental strain
[c] Exact insertion site could not be determined
[d] Defined by the two genes at each boundary of the intergenic space. The 67C5 is 217bp downstream of LMON_2430 and 100bp upstream of LMON_2431 while the 33F8 insertion is 7bp downstream of LMON_1882 and 373bp upstream of LMON _1883

875

876 **Table 3.** Biomass, roughness coefficient, maximum thickness and average thickness of biofilms
877 formed by the wild-type (wt) and the mutants 39G5 (*mltD* mutant) and 44D3 (*mgtB* mutant) in
878 MWB and MWB with a final concentration of 5 mM Mg^{2+} after incubation at 30°C for 7 d
879 calculated using COMSTAT. The standard deviation was calculated from three analysed images
880 taken of each sample and are shown in brackets.

	wt	wt-Mg^{2+}	39G5	39G5-Mg^{2+}	44D3	44D3-Mg^{2+}
Biomass ($\mu m^3/\mu m^2$)	1.145	0.497	1.813	0.191	0.841	1.626
	(0.054)	(0.409)	(1.620)	(0.043)	(1.130)	(0.950)
Roughness coefficient (Ra*)	0.639	1.515	0.891	1.787	1.284	0.654
	(0.074)	(0.256)	(0.750)	(0.009)	(0.874)	(0.455)
Maximum thickness (µm)	4.784	4.951	9.162	4.280	10.966	5.077
	(1.452)	(0.317)	(3.767)	(0.00)	(6.764)	(0.262)
Average thickness	2.295	0.840	4.063	0.320	3.107	2.398
(Entire area) (µm)	(0.776)	(0.561)	(2.399)	(0.089)	(4.807)	(1.340)
Average thickness (Biomass)	3.357	3.281	7.408	3.026	4.904	3.238
(µm)	(1.377)	(0.533)	(2.243)	(0.913)	(4.283)	(1.082)

881 **Table 4**. Primers used in this study.

Primer name	Nucleotide sequence of primer (5'-3')	Product size	Reference	Usage
uvrB_Fwd	CAA*CTGCAG*CCTTCAATTAAATCCACATCTGGT (*Pst*I)	2528	This study	Complementation of 33E11
uvrB_Rev	AAC*GGATCC*TGTGCTTGCAACGTATATGCT (*Bam*HI)		This study	
mltD_Fwd	CAA*CTGCAG*TTGACGTAGAAACACCTTAGCAC (*Pst*I)	2683	This study	Complementation of 39G5
mltD_ Rev	AAC*GGATCC*AAAGGCAATTTCGGTGCGAC (*Bam*HI)		This study	
16S_Fwd	CAGCAGCCGCGGTAATAC	938	(87)	Identification of *Listeria monocytogenes*
16S_Rev	CTCCATAAAGGTGACCCT		(87)	
Marq254	CGTGGAATACGGGTTTGCTAAAAG		(76)	Arbitrary PCR
Marq255	CAGTACAATCTGCTCTGATGCCGCATAGTT		(76)	
Marq206	TGTCAGACATATGGGCACACGAAAAACAAGT		(76)	
Marq207	GGCCACGCGTCGACTAGTACNNNNNNNNNGTAAT		(76)	
Marq208	GGCCACGCGTCGACTAGTAC		(76)	
Marq257	CTTACAGACAAGCTGTGACCGTCT		(76)	
Marq270	TGTGAAATACCGCACAGATGCGAAGGGCGA		(76)	
Marq271	GGGAATCATTTGAAGGTTGGTACT		(76)	
T7promoter	TAATACGACTCACTATAGGG		Macrogen, Inc (South Korea)	Presence of vector pIMK

882 Italics represent restriction enzyme sites; used restriction enzymes are shown in brackets; N= A or C or G or T

883

Figures

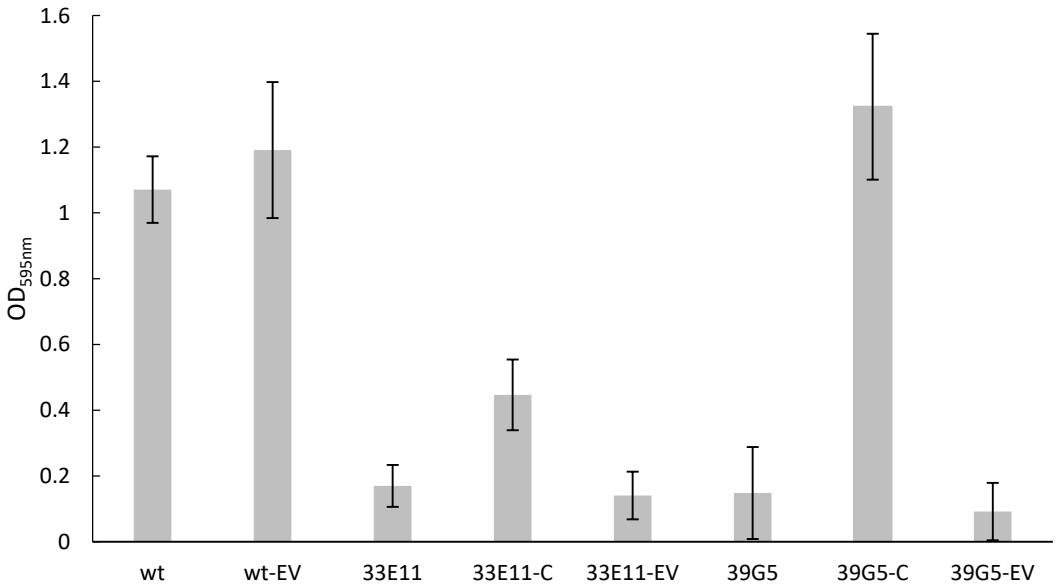

Figure 1. A comparison of biofilm formation in *Listeria monocytogenes* 15G01 (wt), the *uvrB* and *mltD* mutants (33E11 and 39G5), and mutants containing a wild type copy of the corresponding gene (complemented strains (-C)) or the empty vector pIMK (-EV). Error bars represent the standard deviation for three independent experiments (n=6). Biofilm formation was determined by measuring the OD_{595nm} as part of the CV assay.

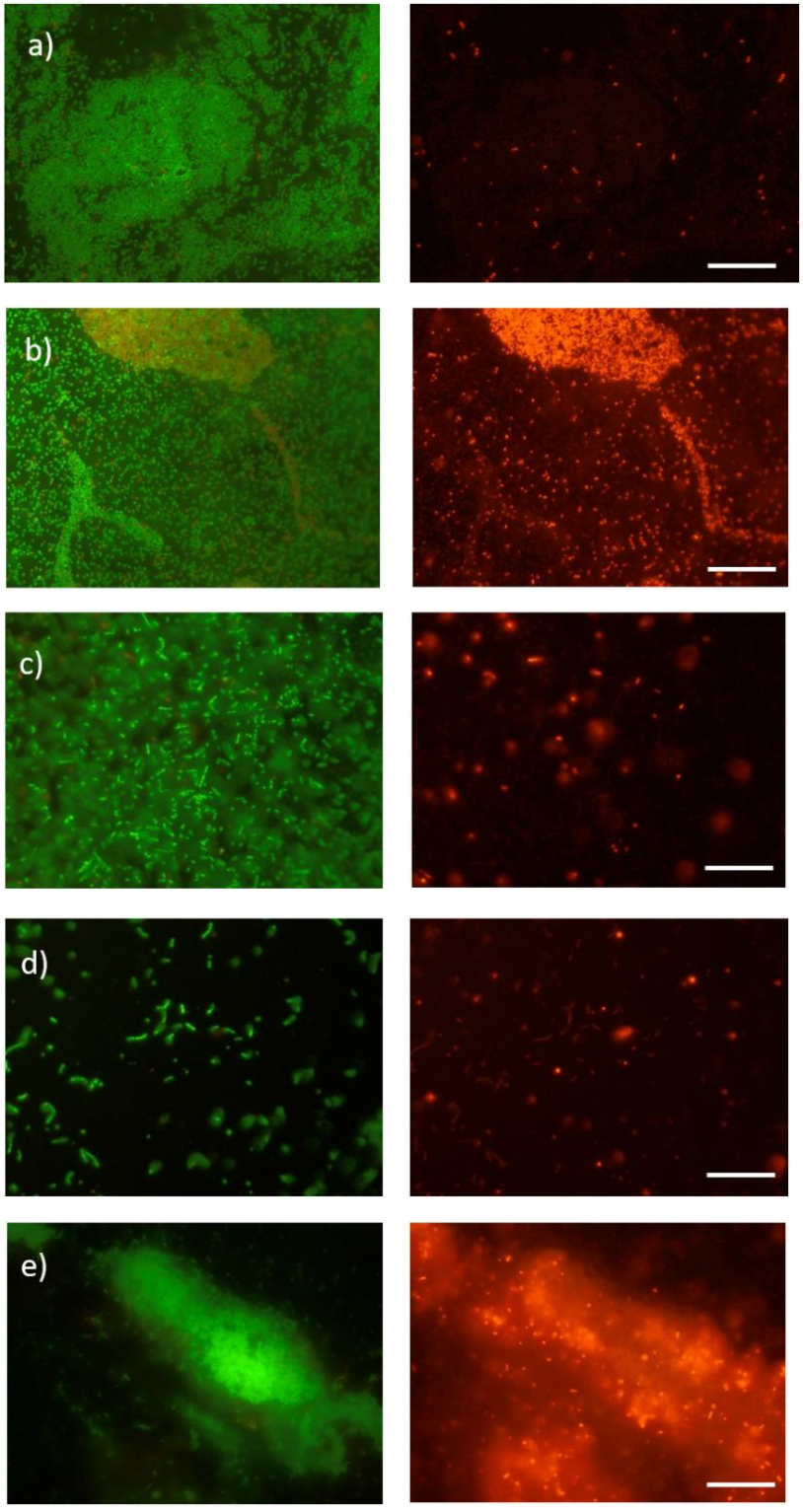

892

893 **Figure 2.** Images of the biofilms produced by *Listeria monocytogenes* 15G01 (wild-type) (a) and

894 selected transposon mutants with altered biofilm formation (34F11 (b), 33E11 (c), 39G5 (d) and

895 44D3 (e)) grown on polystyrene surfaces in MWB for 48 h at 30°C. The biofilms were stained

with the LIVE/DEAD *Bac*Light bacterial viability kit according to the manufacturer's instruction (Life Technologies, Thermo Fisher, New Zealand). Living cells were labelled with SYTO9 (green) and dead cells with propidium iodide (red). Scale bars represent 20 µm.

34F11 – *clsA* mutant

33E11 – *uvrB* mutant

39G5 – *mltD* mutant

44D3 – *mgtB* mutant

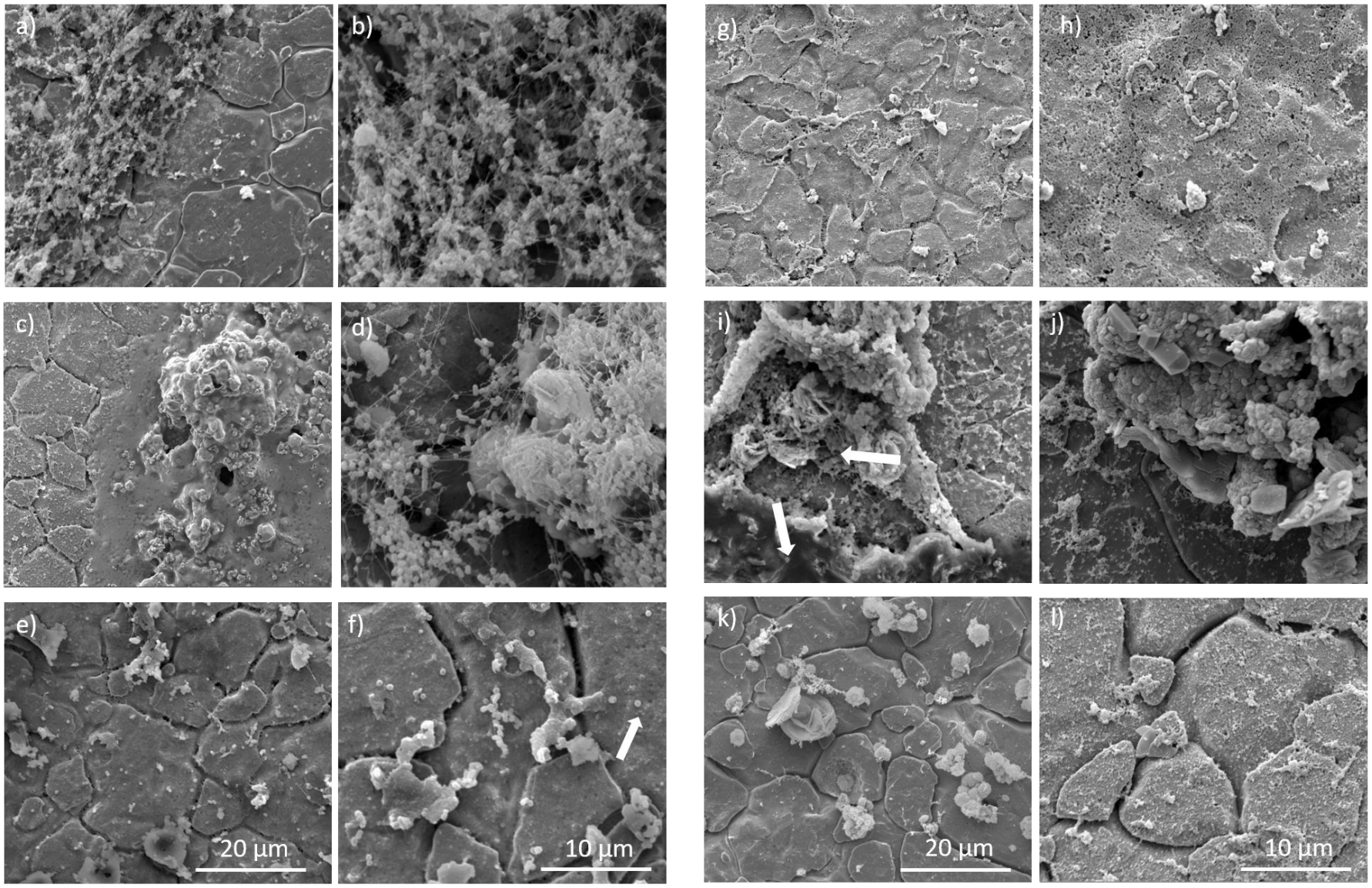

903

Figure 3. Images of the coupon coated with mussel juice (k and l) and the biofilms produced by *Listeria monocytogenes* 15G01 (wild-type) (a and b) and selected transposon mutants with altered biofilm formation (34F11 – *clsA* mutant (c and d), 33E11 – *uvrB* mutant (e and f), 39G5 – *mltD* mutant (g and h) and 44D3 – *mgtB* mutant (i and j)) grown on stainless steel coupons coated with mussel juice for 7 d at 30°C. The images were obtained with a scanning electron microscope with 5000x and 10,000x magnification. The cracks are features of the stainless steel surface. The white arrows point at coccoid-shaped bacteria (f) and the two different types of biofilm (i).

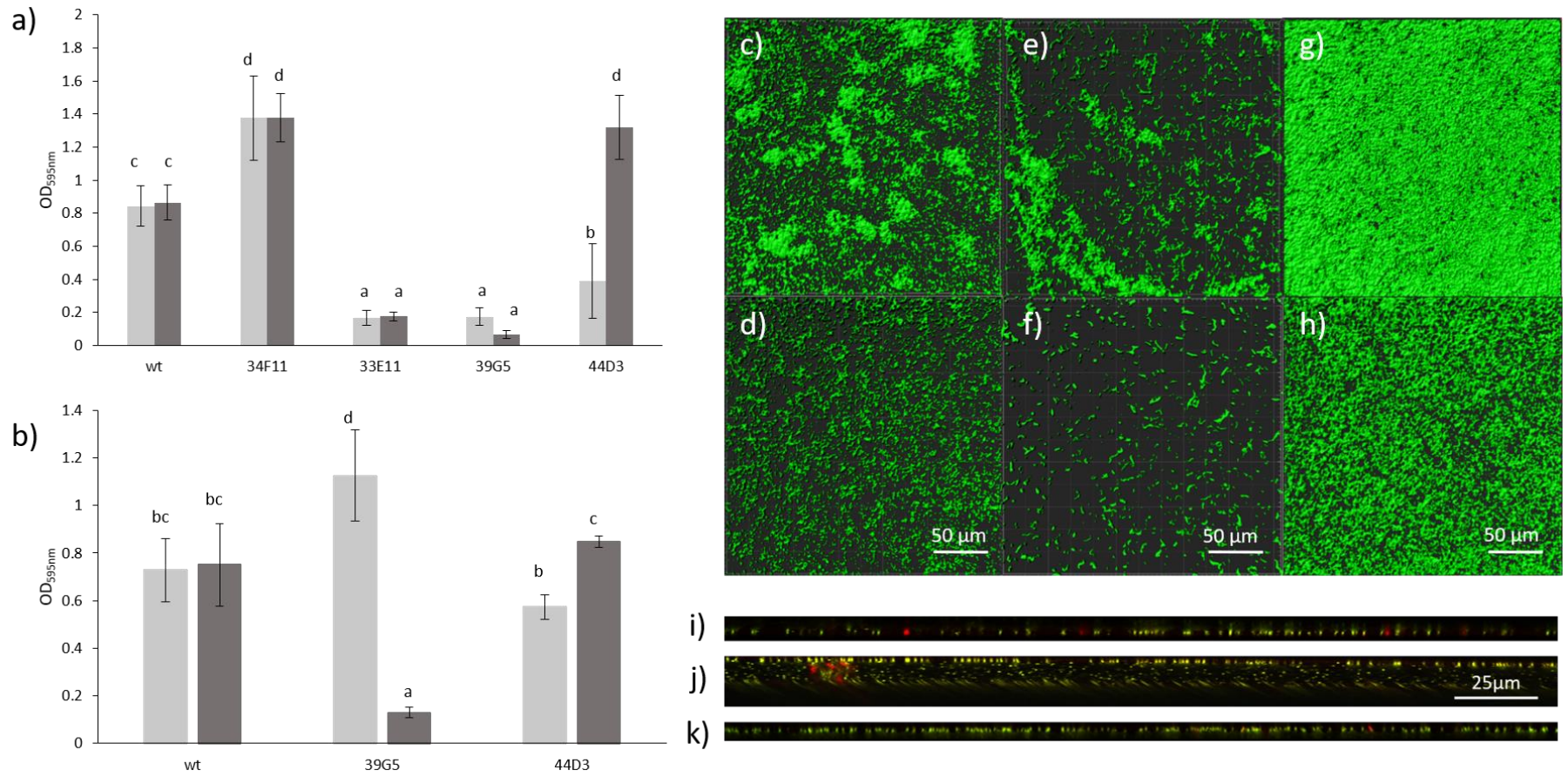

912

913 **Figure 4.** Biofilm formation of the wild-type and selected mutants in MWB (light grey bars) and MWB with a Mg^{2+} concentration of 5

914 mM (dark grey bars) at 30°C (a) and 37°C (b) after 48 h of incubation measured with the CV-assay. Error bars represent standard

915 deviation of three independent experiments (n=6). Letters in common indicate no significant difference.

Isosurface images of biofilms of the wild-type (c), 39G5 (e) and 44D3 (g) formed on glass after 7 d incubation in MWB (1.67 mM Mg^{2+}) and in MWB with a final Mg^{2+} concentration of 5 mM (wild-type (d), 39G5 (f) and 44D3 (h)). Biofilms were grown at 30°C (wild-type, 44D3) or 37°C (39G5) and stained with SYTO9.

Orthogonal view of biofilms formed on a glass surface after 7 d at 30°C by the wild-type in MWB (i), by the *mgt*B mutant (44D3) in MWB (j) and by the *mgtB* mutant (44D3) in presence of 5 mM Mg^{2+} (k). Images were taken after removal of media and staining with the LIVE/DEAD *Bac*Light kit with a confocal laser scanning microscope.

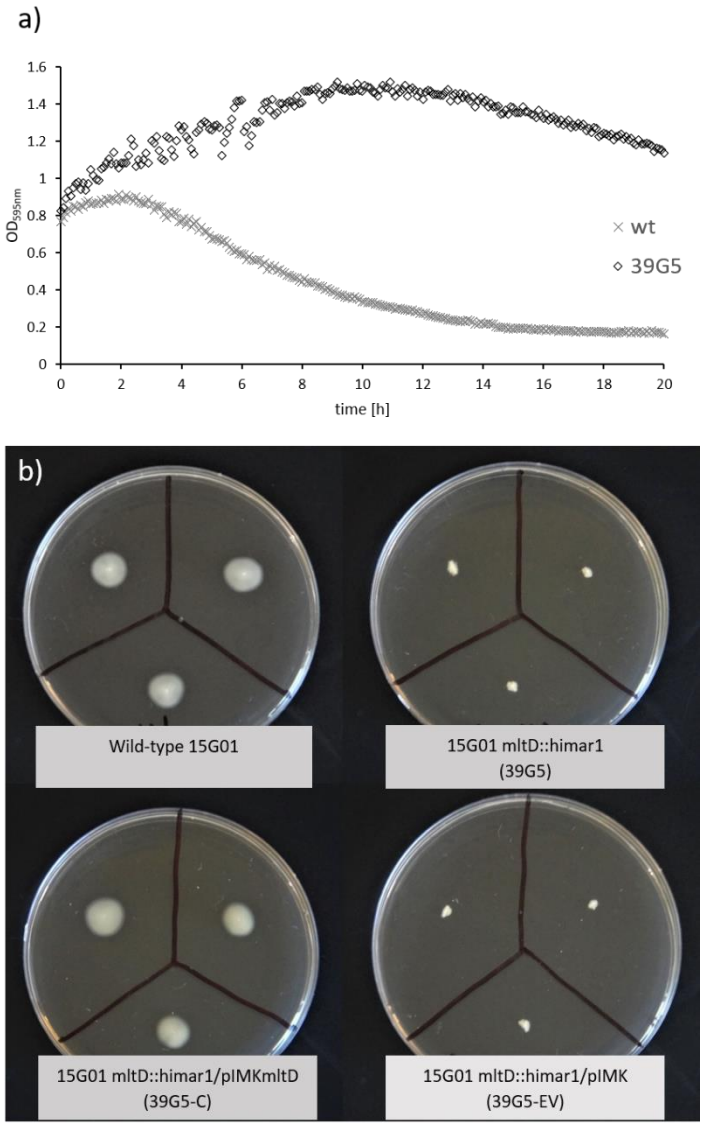

Figure 5. (a) Triton X-100 induced autolysis of *Listeria monocytogenes* 15G01 (wt) and the *mltD* mutant (39G5) determined by optical density measurement at 595nm and (b) motility of *L. monocytogenes* 15G01 (top left), the *mltD* mutant (*39G5 –top right*) and the *mltD* mutant containing a wild-type copy of the corresponding gene (39G5 -C bottom left) or the empty vector pIMK (39G5-EV bottom right) after 24 h at 30°C.

931

932

Supplementary information

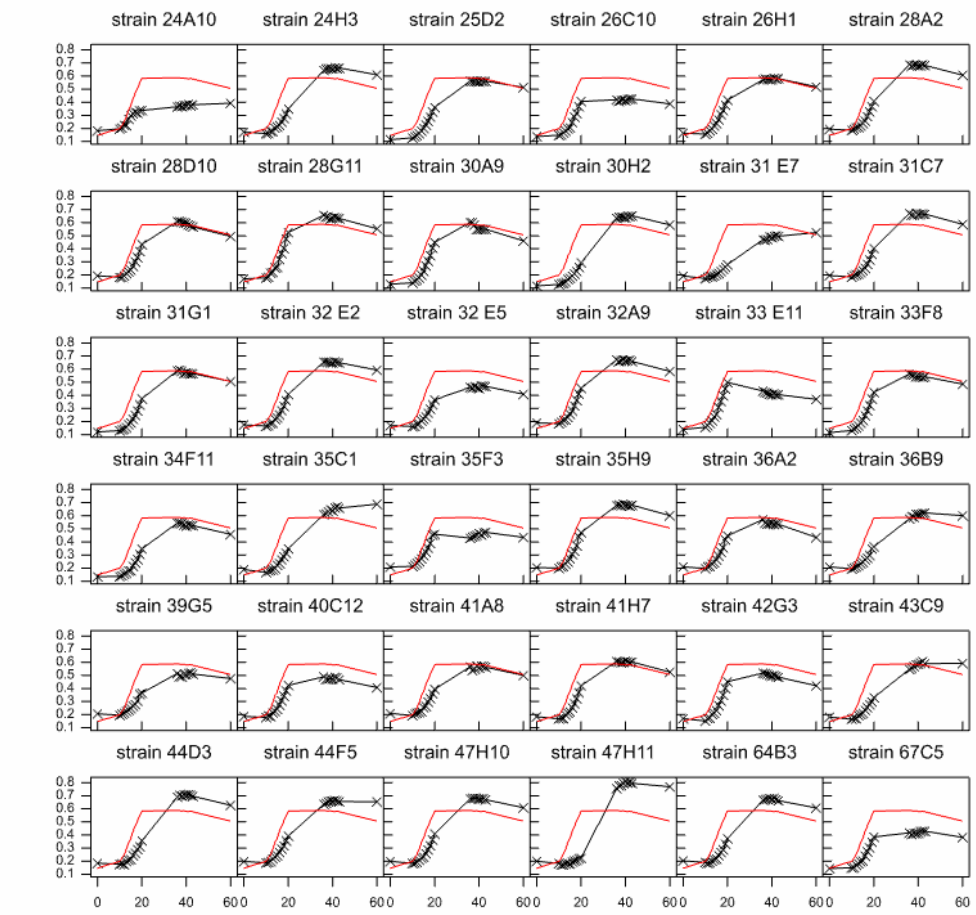

Supplementary Figure S1. Growth of 36 transposon mutants of the *Listeria monocytogenes* 15G01 strain in MWB at 30°C determined by optical density measurements at 595 nm. A 96-well plate with each well containing 200 µL of MWB was inoculated with an overnight culture of *L. monocytogenes* 15G01 and mutants grown in TSBYE at 37°C using a 96-well replicator. The turbidity of the wells was measured with a microplate reader at a wavelength of 595 nm at given time points. The readings were averaged and plotted against measured time points to produce a growth curve. OD_{595nm} values of the samples were corrected by subtracting the OD_{595nm} values for uninoculated media. The wild-type growth curve is shown in red.

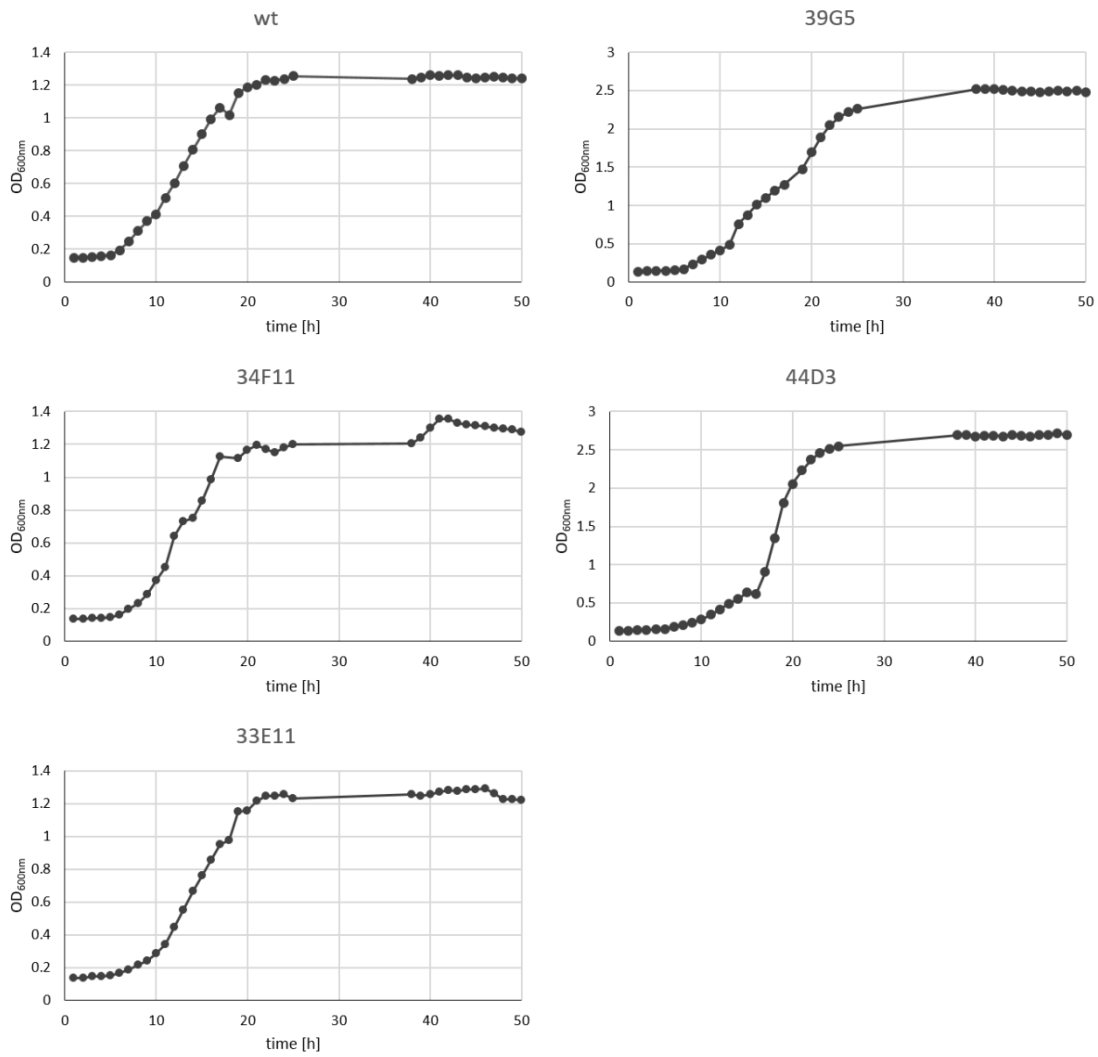

Supplementary Figure S2. Growth of the *Listeria monocytogenes* strain 15G01 (wt) and its four mutants in MWB at 30°C measured with an automated microplate reader at defined time points at 600 nm. The mutants have been grown without selective antibiotics to eliminate its effects on growth. The growth curves pictured are the means of two measurements.

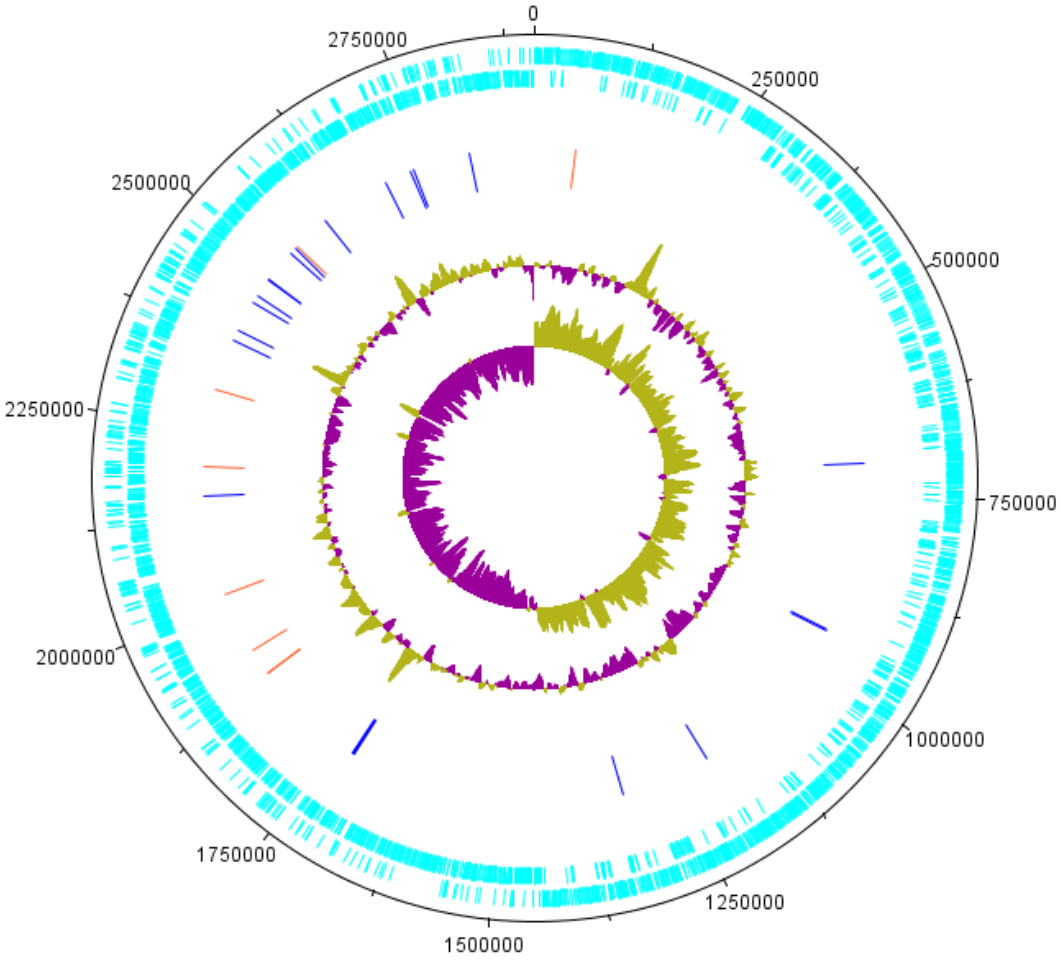

Supplementary Figure S3a. A representation of the genome of *Listeria monocytogenes* EGD showing the locations of transposon insertion sites associated with biofilm formation in *L. monocytogenes* 15G01. The outer ring represents the scale in bp, protein coding sequences are shown in turquoise, the middle ring highlights genes with a transposon insertion leading to greater biofilm formation (orange) and low biofilm formation (blue) in 15G01 and the inner ring (purple/green) shows the G+C % content plot with the GC skew. The image was generated using DNAPlotter (version 1.11) available from www.sanger.ac.uk.

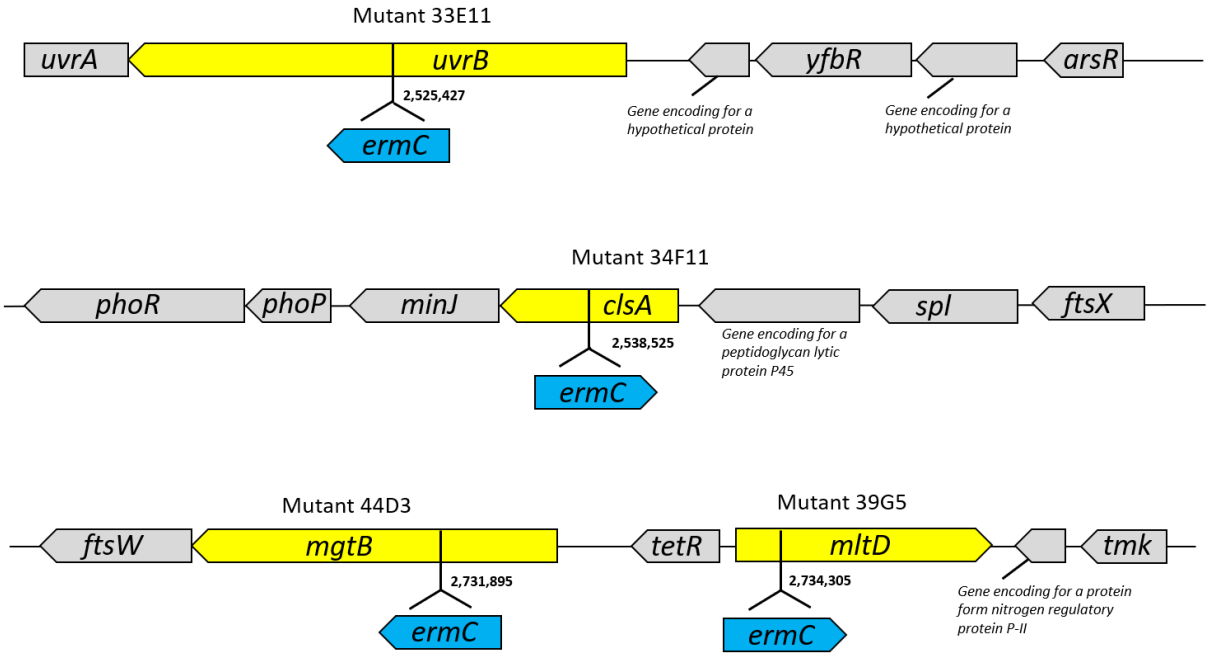

Supplementary Figure S3b. Co-ordinates of the transposon insertions of the four genes hit by the transposon in *L. monocytogenes* 15G01.

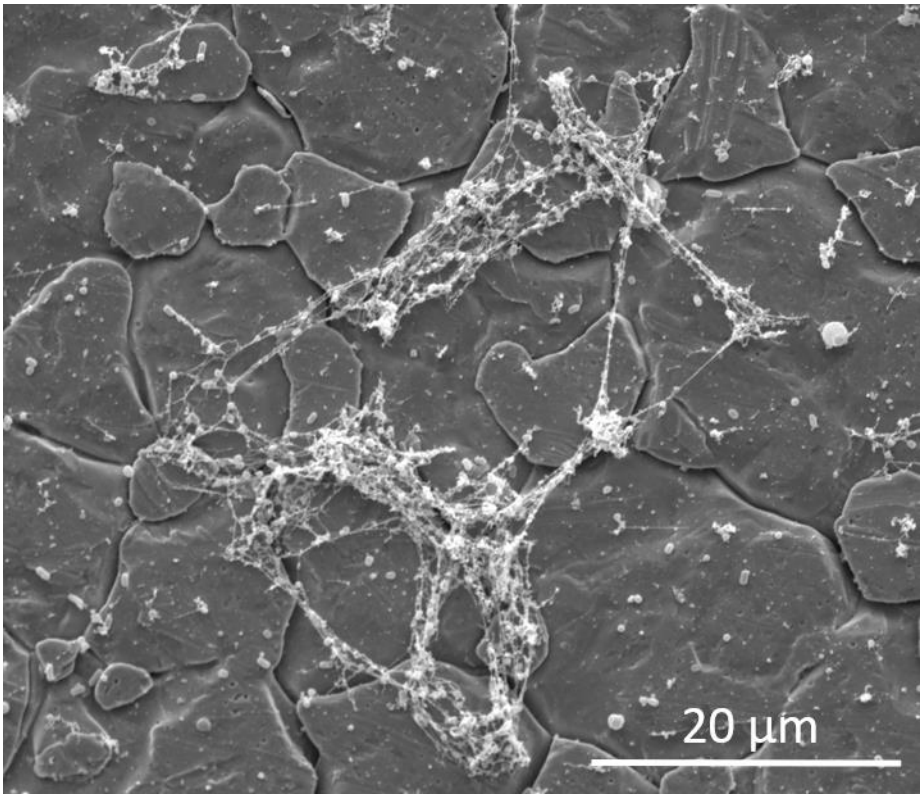

Supplementary Figure S4. Scanning electron microscopy image of a biofilm formed by the *flaA* mutant (41H7) after 7 d incubation at 30°C on stainless steel coupons coated with mussel juice at a 5000x magnification.

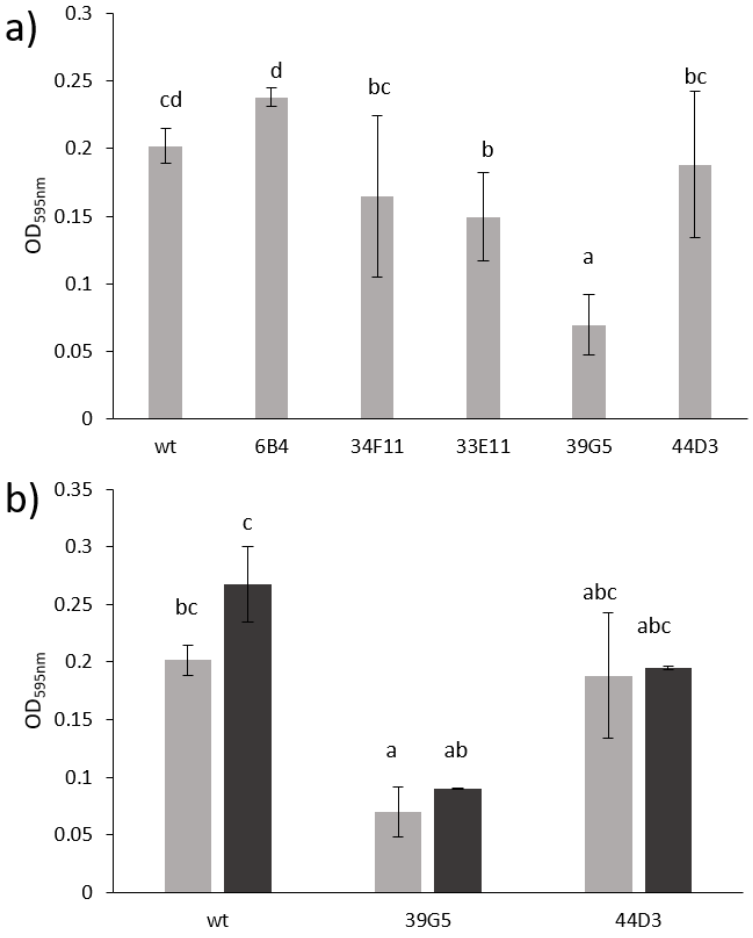

Supplementary Figure S5. Attachment of the *Listeria monocytogenes* 15G01 (wt) strain and the five mutant strains on polystyrene after 30 min at 30°C in MWB (a) and attachment of *L. monocytogenes* 15G01 (wt) and the mutants in MWB (light grey bars) and in MWB-5mM Mg^{2+} (dark grey bars) (b). Error bars represent the standard deviation of two experiments with n=12. Letters in common indicate no significant difference.

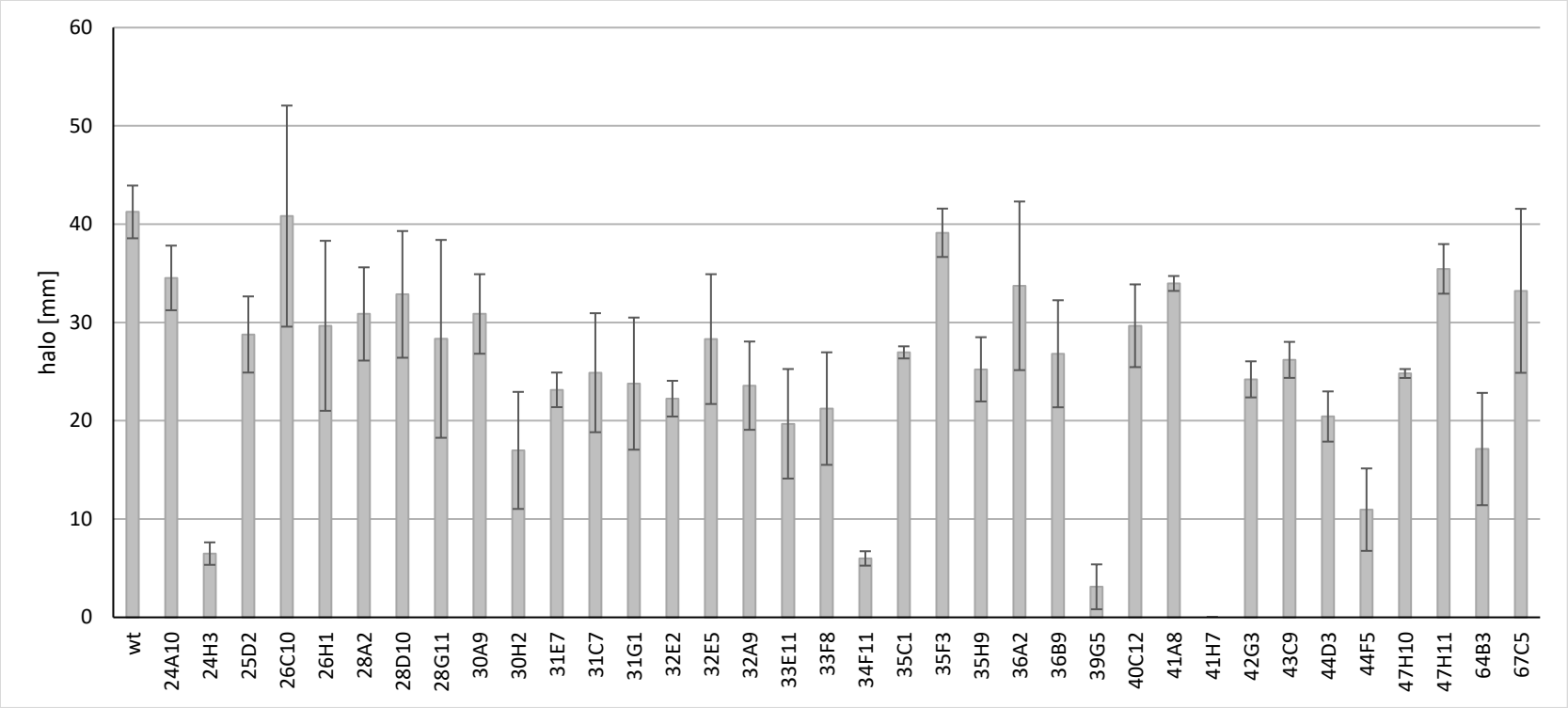

Supplementary Figure S6. Motility of the *Listeria monocytogenes* 15G01 (wt) strain and the 36 mutant strains after 48 h of incubation at 30°C measured as halo produced in TSA+0.25% agar. The error bars represent standard deviations of three independent experiments carried out with three replicates each.

Supplementary Table S1. Growth of 36 transposon mutants of the *Listeria monocytogenes* 15G01 strain in MWB at 30°C determined by optical density measurements at 595 nm.

To compare the mutant strains to the wild-type, logistic growth curves were fitted to each repetition of each strain (using the FITCURVE procedure in Genstat version 17, 2014). Because of the declines noted for some strains at 60 h, the 60 h data were excluded. The parameters of the curves were then compared to those for the wild-type replicates using t-tests.

All the strains were significantly different from the wild-type on at least one parameter. The most consistent difference was that all but two strains (24A10 and 33E11) had significantly higher m. The other notable feature was that most strains grew slower (lower b) than the wild-type, which is quite likely due to antibiotic presence.

The mean parameters (from the eight repetitions) are tabulated below, along with standard errors (s.e — based on the difference between the repetitions) and p values for the difference from the wild-type. P values are colour coded yellow (significant at p = 0.05 and value is higher than the wild-type) and turquoise (significant at p = 0.05 and value is lower than the wild-type).

	a (starting level)			Slope at time = m			c (how much line rises)			m (midpoint of increasing phase)		
Strain	Mean	s.e.	p	Mean	s.e.	p	Mean	s.e.	p	Mean	s.e.	p
Wild-type	0.15	0.004		0.053	0.001		0.44	0.012		14.6	0.55	
24A10	0.17	0.001	<.001	0.021	0.001	<.001	0.20	0.001	<.001	14.5	0.34	0.949
24H3	0.16	0.003	0.066	0.043	0.001	<.001	0.50	0.009	0.001	21.4	0.21	<.001
25D2	0.11	0.002	<.001	0.037	0.001	<.001	0.45	0.011	0.459	19.3	0.20	<.001
26C10	0.15	0.005	0.989	0.043	0.002	0.004	0.27	0.002	<.001	17.0	0.39	0.003
26H1	0.15	0.001	0.589	0.040	0.001	<.001	0.43	0.008	0.404	18.6	0.15	<.001
28A2	0.19	0.001	<.001	0.049	0.001	0.108	0.50	0.011	0.002	20.5	0.31	<.001
28D12	0.18	0.002	<.001	0.048	0.001	0.013	0.41	0.006	0.056	19.1	0.33	<.001
28G11	0.17	0.004	0.001	0.054	0.001	0.374	0.47	0.011	0.086	17.8	0.12	0.001
30A9	0.13	0.003	0.002	0.048	0.001	0.015	0.44	0.006	0.889	17.8	0.24	<.001
30H2	0.11	0.004	<.001	0.036	0.001	<.001	0.54	0.004	<.001	22.9	0.50	<.001
31 E7	0.17	0.003	<.001	0.022	0.002	<.001	0.32	0.011	<.001	23.1	0.60	<.001
31C7	0.19	0.002	<.001	0.050	0.001	0.123	0.48	0.006	0.009	20.5	0.32	<.001
31G1	0.12	0.002	<.001	0.046	0.001	0.001	0.45	0.004	0.211	19.5	0.53	<.001
32 E2	0.16	0.004	0.032	0.047	0.001	0.006	0.49	0.011	0.006	20.0	0.21	<.001
32 E5	0.16	0.003	0.019	0.034	0.001	<.001	0.30	0.005	<.001	18.5	0.28	<.001
32A9	0.18	0.001	<.001	0.049	0.001	0.071	0.48	0.007	0.005	19.3	0.18	<.001
33 E11	0.16	0.002	0.020	0.055	0.001	0.220	0.27	0.011	<.001	15.5	0.08	0.151
33F8	0.12	0.003	<.001	0.045	0.002	0.003	0.43	0.014	0.589	18.1	0.14	<.001
34F11	0.13	0.003	0.004	0.038	0.001	<.001	0.40	0.010	0.034	19.7	0.25	<.001
35C1	0.16	0.004	0.050	0.035	0.002	<.001	0.49	0.006	0.002	22.0	0.41	<.001
35F3	0.22	0.002	<.001	0.040	0.000	<.001	0.24	0.003	<.001	16.2	0.14	0.025
35H9	0.20	0.003	<.001	0.052	0.001	0.818	0.49	0.009	0.007	19.2	0.41	<.001
36A2	0.20	0.002	<.001	0.044	0.001	<.001	0.34	0.004	<.001	18.2	0.32	<.001

36B9	0.19	0.002	<.001	0.034	0.001	<.001	0.41	0.010	0.135	21.0	0.13	<.001
39G5	0.20	0.002	<.001	0.031	0.001	<.001	0.31	0.010	<.001	19.4	0.18	<.001
40C12	0.18	0.003	<.001	0.039	0.001	<.001	0.30	0.009	<.001	17.5	0.40	0.001
41A8	0.20	0.003	<.001	0.038	0.001	<.001	0.36	0.003	<.001	19.5	0.20	<.001
41H7	0.17	0.001	0.001	0.050	0.001	0.084	0.43	0.007	0.756	19.3	0.29	<.001
42G3	0.16	0.007	0.296	0.045	0.003	0.044	0.35	0.013	<.001	17.4	0.23	0.001
43C9	0.16	0.003	0.115	0.030	0.002	<.001	0.43	0.009	0.496	21.8	0.50	<.001
44D3	0.17	0.002	<.001	0.044	0.001	<.001	0.53	0.006	<.001	22.0	0.42	<.001
44F5	0.18	0.004	<.001	0.040	0.001	<.001	0.47	0.017	0.112	20.7	0.18	<.001
47H10	0.18	0.002	<.001	0.050	0.001	0.194	0.49	0.008	0.002	20.4	0.26	<.001
47H11	0.18	0.003	<.001	0.050	0.000	0.104	0.63	0.009	<.001	28.1	0.33	<.001
64B3	0.19	0.003	<.001	0.051	0.001	0.449	0.49	0.006	0.003	21.1	0.23	<.001
67C5	0.15	0.004	0.858	0.038	0.002	<.001	0.27	0.003	<.001	17.3	0.32	0.001